ESTIMATION OF EVAPOTRANSPIRATION FROM AIRBORNE HYPERSPECTRAL SCANNER DATA USING THE SCOPE MODEL

ASMAA MAHMOUD AHMED ABD EL BAKI

February, 2013

SUPERVISORS:

First Supervisor Prof. Dr. ing. W. (Wouter) Verhoef

Second Supervisor Dr. ir. C. (Christiaan) van der Tol

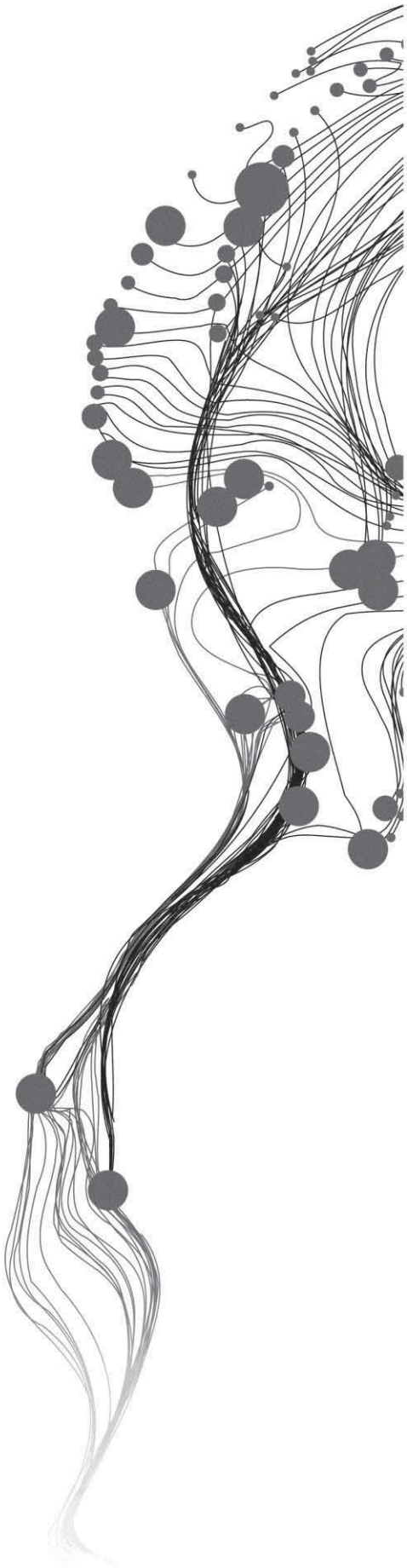

ESTIMATION OF EVAPOTRANSPIRATION FROM AIRBORNE HYPERSPECTRAL SCANNER DATA USING THE SCOPE MODEL

ASMAA MAHMOUD AHMED ABD EL BAKI

Enschede, The Netherlands, February, 2013

Thesis submitted to the Faculty of Geo-Information Science and Earth Observation of the University of Twente in partial fulfilment of the requirements for the degree of Master of Science in Geo-information Science and Earth Observation.
Specialization: Water Resources and Environment Management

SUPERVISORS:

First Supervisor Prof. Dr. ing. W. (Wouter) Verhoef

Second Supervisor Dr. ir. C. (Christiaan) van der Tol

THESIS ASSESSMENT BOARD

Chairman Dr. ir. M.W. (Maciek) Lubczynski

External Examiner Dr. Ir. J.G.P.W. Clevers, Wageningen University

INTERNATIONAL INSTITUTE FOR GEO-INFORMATION SCIENCE AND EARTH OBSERVATION
ENSCHEDE, THE NETHERLANDS

DISCLAIMER

This document describes work undertaken as part of a programme of study at the Faculty of Geo-Information Science and Earth Observation of the University of Twente. All views and opinions expressed therein remain the sole responsibility of the author, and do not necessarily represent those of the Faculty.

ABSTRACT

Vegetation dynamics have been recognized in the recent years in which vegetation is a key element influencing evapotranspiration (ET). Evapotranspiration affects significantly the global hydrological cycle. Hence the accurate ET is required in the field of agriculture. The Soil, Canopy Observation, Photochemistry and Energy Balance model (SCOPE) integrates radiative transfer and energy balance model for modelling biophysical processes. Evapotranspiration is one of biophysical processes. SCOPE is a novel model so that calibration and validation must be conducted to ascertain its operational use. In this research, the simulated ET from the SCOPE model was evaluated against ground measurements.

The two processes, calibration and validation, were conducted on grass and camelina grown in Castilla-La Mancha region Barrax, Spain. The calibration process is accomplished by using the spectral information measured from airborne hyperspectral scanner with the spectral information simulated from look-up tables (LUTs) using an inversion approach. The airborne hyperspectral scanner (AHS) of the Spanish Instituto Nacional de Tecnica Aerospacial (INTA) was used to derive biophysical and biochemical parameters over an agriculture area which was recorded on 17th July 2012. The scanner has 80 spectral bands with the high spectral and spatial resolution and covers all spectral information for detecting vegetation status accurately. Selecting the best parameters is based on the lowest error obtained by comparing the spectral information (optical and thermal radiation) generated from modelled LUTs and spectral information measured from AHS data. The atmospheric correction (AC) and geometric correction were applied to the AHS data to retrieve realistic values from measured data. The validation process is achieved by comparing the ET estimated from SCOPE model against eddy covariance flux tower for camelina and lysimeter technique for grass.

The findings of this research revealed that time series of daily ET estimated by the SCOPE model has a good agreement with ground data for grass. However, for camelina it showed a negative correlation and this was due to sudden change of environmental conditions. During estimation of ET from thermal radiation, ET simulated from the SCOPE time series model is different from ET measured for camelina. This is most likely related with the uncertainty of surface emissivity and the skin temperature as well as the insufficient parameterization of surface resistance of vapour transport in soil pores (rss). For grass, modelled and measured time series of ET agree. SCOPE model has high potential for monitoring biophysical process (ET) on local scale by using AHS.

Keywords: Evapotranspiration (ET), airborne hyperspectral scanner (AHS), Soil canopy observation, photochemistry and energy balance (SCOPE), Atmospheric correction (AC).

ACKNOWLEDGEMENTS

First of all, I would greatly thank ALLAH for achieving my success and dreams. Without your blessings, I am completely lost and incapable.

I would like to thank the Erasmus Mundus Programme of the European Union for granting me the opportunity to study in WREM department 2012-2013 and gain a lot of knowledge form all stuff.

I want to express my sincere gratitude to my supervisors, Prof. Dr. Wouter Verhoef and Dr. Christiaan van der Tol, since they are teaching me a lot, supporting me all the time, advising and giving me critical comments during the conduct of this research. Without them, this research couldn't be done. I would like thank Dr. Joris Timmermans for helping and supporting me.

I am grateful to all my classmates for providing me with love and supporting during 18 months. I wish for them success in their future life and hope one day we can meet again especially for Tahani ahmed, Melakau estifanos, Ali naeini, Ahmed abd el hamid, Ftama elsafoury, Hifa mohsen, Samaneh khaef, Derrick mario, Tsitsi bangeria.

I deeply appreciate the support of Mr. Omar. mohamed PhD student who assisted me for sharing with me insightful knowledge and giving me critical comments during the research. I wish for him Allah help him to achieve his successes and ambitions in his life.

Many thanks to beloved my family especially my mother and my father for encouraging me all the time and for their prayers. God protect them and give them health and happiness.

Finally, thank to the Regional Experiments for Land-atmosphere Exchanges (REFLEX) campaign, they were provided the dataset of AHS and field measurements for achieving the objectives of my research.

TABLE OF CONTENTS

LIST OF FIGURES

LIST OF TABLES

LIST OF ABBREVIATIONS AND ACRONYMS

AC	Atmospheric correction
ATCOR4	Atmospheric & Topographic Correction
AFRL	Air Force Research Laboratory
ANN	Artificial Neutral Network
ASD	Spectroradiometers
AOT	Aerosol Optical Thickness
AHS	Airborne Hyper-spectral Scanner
AVHRR	Advanced Very High Resolution Radiometer
AVIRSI	Airborne Visible / Infrared Imaging Spectrometer
CASI	Compact Airborne Spectrographic imager
C_s	Senescent material
C_m	Dry matter content
C_{ab}	Chlorophyll a+b content
C_w	Equivalent water thickness
EC	Eddy covariance technique
ea	Vapour pressure
ET	Evapotranspiration
ε	Emissivity
fAPAR	Fraction of Absorbed Photosynthetically Active Radiation
FWHM	Full width half maximum
IFOV	Instantaneous field of view
FluorSAIL	Optical properties chlorophyll fluorescence on canopy model
G_b	Gain factor of background
G_t	Gain factor of target
$GRFL_{50}$	Total ground reflectance radiance contribution at surface albedo 0.5
$GRFL_{100}$	Total ground reflectance radiance contribution at surface albedo 1
HyMap	Hyperspectral Mapper
INTA	Instituto Nacional de Técnica Aeroespacial, Spain
ITAP	Instituto Técnico Agronómico Provincial de Albacete, Spain
IGM	Image Geometry Map
LUT	Look Up Table
La (b)	The atmosphere path thermal radiation at BOA(bottom of atmosphere)
La (t)	the atmospheric path thermal radiance at TOA (top of atmosphere)
LADF(a+b)	Leaf angle distribution function for spherical
Ls	Radiance from surface
$\overline{L}$	Average radiance over the whole scene
L_0	Atmospheric path radiance
LAI	Leaf area index
MODTRAN 5.2.1	(MODerate spectral resolution atmospheric TRANSmittance algorithm and computer model).
MIR	Medium InfraRed (3.0 to 5.0 micrometer)
MSS	Multispectral Scanner
m	Bell-Barry parameter

n	Number of bands
N	Leaf structure parameter
NRL	Naval Research Laboratory
PROSPECT	Leaf optical properties
PTEM	Path thermal radiation at surface albedo 0
rbs	Boundary layer resistance of soil
rss	Surface resistance of vapour transport in soil pores
rwc	Aerodynamic resistance within Canopy
r_t	Reflectance from target
RTM	Radiative transfer model
RTMo	Radiative transfer model of solar and sky radiation
RTMt	Radiative transfer model of emitted by vegetation and soil
RTMf	Radiative transfer model of fluorescence
Rli	Incoming radiation of long wave
Rsi	Incoming radiation of short wave
REFLEX	Regional Experiments for Land-atmosphere Exchange
RAA	Relative azimuth angle
S	Spherical albedo from ground
SWIR	Short Wave InfraRed
SCOPE	Soil Canopy Observation, Photochemistry and Energy fluxes
SAIL	Scattering by Arbitrarily Inclined Leaves model
SZA	Solar Zenith Angle
SKYL	Ration of diffuse to total incident radiation
SVAT	Soil-vegetation-atmosphere-transfer model
SPOT	Système Pour l'Observation de la Terre
TIR	Thermal InfraRed
TM	Thematic Mapper
TOA	Top of atmosphere
TOC	Top of Canopy
TRAN	Direct transmittance from target to sensor
TES	Temperature and Emissivity Separation algorithm
UTM	Universal Transverse Mercator
VZA	Viewing zenith angle
VIS	Visible
VNIR	Visible Near InfraRed
Vmax	Maximum carboxylation capacity rate
WGS84	World Geodetic System 1984

1. INTRODUCTION

1.1. Background

Evapotranspiration (ET) is a key biophysical process of vegetation for the estimation of relationships between vegetation canopy, soil and atmosphere. Where evapotranspiration affects significantly the global hydrological cycle and the energy balance, it represents the water loss to the atmosphere by two processes: evaporation and transpiration. Changes in ET through time and space provide important information about land surface processes. In the field of agriculture, assessment of actual evapotranspiration is necessary to compute net water volumes and the net irrigation volume.

The importance of studying vegetation dynamics has been recognized in the recent years (Box, 1978; Ito, 2011). Vegetation is a very important key element influencing ET. That is mainly because of its direct effect on the energy transfer between the earth surface and the atmosphere via many variables such as plant type, plant growth stage and level of maturity. Soil moisture content and weather conditions have significant effect as well. Different types of plants have their own physiological nature such as expressed by their leaf area index, water content, dry matter of plant, stomatal resistance, chlorophyll content and root depth which are affecting the evapotranspiration process.

Nowadays, many scientists have been working on techniques for retrieving accurately the amount of evapotranspiration. Remote sensing can aid to resolve this challenging problem. Remote sensing imagery of various spatial resolutions can assist in providing important information about biophysical processes from regional scale to global scale by using different types of satellites. Many kinds of satellite data, starting with NASA's MSS launched in 1972, TM launched in 1984, NOAA's AVHRR launched in 1978 and the SPOT satellites have a limited number of bands, and critical information available in specific narrowband and may not be detected(Cho, 2007) to study the spatial and temporal variability of many ecosystems and environmental conditions(Zarco-Tejada et al., 2007). On the contrary, hyperspectral remote sensing has many bands, and thus provides more information about vegetation. Monitoring of biochemical and biophysical parameters is possible with sensors such as AHS and CASI (Cho, 2007). All biophysical processes including evapotranspiration, photosynthesis and chlorophyll fluorescence are very important for diagnostics of crop status and for wide range of applications such as weather forecasting (Wetzel et al., 1988), climate change (Destouni et al., 2009)and sustainable water resources (Allen et al., 1998).

(Qi et al., 2000) stated that although remote sensing products in recent years are becoming numerous, remote sensing algorithms based on converting radiometric measurement into biophysical and biochemical variables are still facing problems due to the different scales among remote sensing data and models.

Selecting the most appropriate remote sensing algorithm is an important step to estimate ET. Developing models is important in order to effectively use remote sensing for ET estimation. Models have been built to describe the physical relationships between reflectance spectra and biophysical parameters. Numerous studies have been conducted using models which have been improved significantly in order to use remote sensing data as inputs for estimating fluxes (Zhan et al., 1996)to figure out the interaction between land

surface and atmosphere in terms of water, heat and carbon dioxide fluxes as a function of vegetation structure.

Modelling of radiative transfer started already 30 years ago passing through many stages from simple algorithms to more complex models. The radiative transfer model describes the physical phenomenon of energy transfer in the form of electromagnetic radiation. Light propagation through the medium is one of the most important environmental factors and it is affected by absorption, emission and scattering processes to be included in functional structural models of plants (Combes et al., 2008). Consequently, a successful model could provide absolute information about vegetation, which is highly recommended in terms of widespread applications for ecological or agricultural issues (Baret et al., 2000).

This sequence of developing models treats the canopy as following:
1) big-leaf model (Monteith, 1981).
2) two-layer systems (plant/soil) (Shuttleworth et al., 1985).
3) dual-source system (sun/shade) (dePury et al., 1997; Wang et al., 1998).
4) two-layer/dual source (plant/soil, sun/shade) (Sinclair et al., 1976).
5) One-dimensional multi-layer system (Baldocchi et al., 1995; Goudriaan, 1977).
6) Two-dimensional array (Chen et al., 2008).
7) SCOPE model (soil-canopy observation photochemistry and energy balance) (van der Tol et al., 2009).
8) Three-dimensional array (Kobayashi et al., 2012; Medlyn, 2004; Wang et al., 1990).

In this research, the SCOPE model is used for employing remote sensing with high spectral resolution to retrieve biophysical information since it has the ability of integrating the energy balance and a radiative transfer model.

1.2. Soil-canopy spectral radiances, photosynthesis, fluroscence, temperature and energy balance (SCOPE).

The biophysical model used in this research is the soil canopy observation of photochemistry and energy balance (SCOPE) model which was developed by (van der Tol et al., 2009)at the ITC International Institute for Geo-Information Science and Earth Observation in The Netherlands, in the framework of the ECO-RTM project, funded by the Netherlands Organization for Scientific Research (NWO-SRON-EO71).

The SCOPE model incorporates PROSPECT the leaf optical model, an energy balance model, and the SAIL canopy reflectance model which is integrated radiative transfer and energy balance vertically (1-D). SCOPE has been built into Matlab script. The sub-models of SCOPE are well suited to deal with several aspects of the environmental conditions. Also, each of modules can be used stand-alone or as in the integrated model, depending on applications. The modelling scheme used for simulating water, energy and CO_2 fluxes from leaves level up to atmosphere level (van der Tol et al., 2009).

The main purpose of the new model is connecting optical and thermal radiation from the visible to thermal infrared domain (0.4-50 μm) with high spectral resolution with the purpose of estimating biophysical processes (ET, photosynthesis and chlorophyll fluorescence) (van der Tol et al., 2009). The SCOPE model is a 1D vertical model. It means that it assumes homogeneity in horizontal direction. The main advantages are filling the gap between satellite and flights overpasses to calculate the fluxes from instantaneous data to diurnal cycles and it also works in the absence of remote sensing information especially cloudy days with high accuracy. In addition, it has a potential for validating energy balance

models such as SEBS as ground truth. Moreover it can be used for computing chlorophyll fluorescence from visible part (van der Tol et al., 2009).

1.3. Modelling and inversion

Airborne imaging spectrometers such as AVIRIS or HyMap or CASI and AHS seem to be ideal candidates for monitoring agricultural crops as they provide spectral information with high resolution and high spatial resolutions containing important information on vegetation vitality. Hyperspectral imagery has been successfully applied to examine vegetation health and ecosystem properties in mixed temperature forests (Huber et al., 2008), needle-leaved evergreen forests (Schlerf et al., 2010) and grassland(Darvishzadeh et al., 2008(a)).

Vegetation models can simulate the radiance and reflectance from the canopy which depend on the biochemical and biophysical characteristics of the canopy and the leaves. The model employs hyperspectral images in the inverse mode. There are different inversion techniques such as numerical optimization methods (Jacquemoud et al., 2000; Jacquemoud et al., 1995; Meroni et al., 2004), look-up table (LUT) approach (Combal et al., 2002; Combal et al., 2003; Gastellu-Etchegorry et al., 2003; Weiss et al., 2000) and the artificial neural networks(ANN)approach(Schlerf et al., 2006; Walthall et al., 2004; Weiss et al., 1999). However, advantages and disadvantages of these techniques limit our choice. Generally, the LUT and ANN techniques are more computationally efficient than the numerical optimization method. The LUT method is conceptually the simplest and fast but for large size LUTs, it takes time consuming (Wandera, 2011).

Consequently, in this study, biophysical and biochemical parameters are retrieved from a look up table (LUT) based inversion model, which will be used to generate the simulated spectra from defining the range values of each parameter as interval. Results of using LUT inversion technique within the SCOPE model framework were compared with the airborne data for estimating the best parameters. The best parameters were used as input of the SCOPE to retrieve energy fluxes. These fluxes calculated by the SCOPE model were validated in order to assess the model's ability to represent the processes accurately. It is worth to mention that the best parameters for the SCOPE model differ from one place to another so that model parameterization is required to define parameter ranges applicable to area under study (Goel et al., 2000). The success of the SCOPE model in terms of the output accuracy depends on the resolution of the input data. In this study, images with high spectral resolution; airborne hyperspectral scanner (AHS) was used in order to obtain spectral information. Figure 1-1 presents the general outline of the research work. The details are presented further in this thesis.

1.4. Research justification

The SCOPE model was used in order to estimate accurate values of ET for different land cover. It has ability to retrieve ET from optical and thermal with highly spectral resolution. In addition, the model depends on identification skin temperature for sunlit and shaded plant and soil in vertical dimension. Each plant has different biochemical and biophysical parameters under different conditions so that the model used all these information to retrieve reliable values of ET. During absence remote sensing data, SCOPE time series has capability to quantify fluxes daily based on micrometeorological data. However, SCOPE model needs to calibrate and validate to be applicable in the future and be useful for scientists, irrigation engineers and, farmers. In order to use this model in appropriate way, it is needed to provide accurate input of biophysical and biochemical variables from images as inverse mode by using AHS data.

1.5. Problem statement

Calibration and validation are necessary and critical steps before any model application. SCOPE is a novel model used for estimating biophysical processes from leaf level up to atmosphere. It has not been calibrated to airborne data yet, it has insufficiently been validated. It should be conducting before revealing for wide applications. Thus, this research is targeted mainly to accomplish these processes in a way judging the model performance. Indeed, calibration is basically conducted through adapting and evaluating the model input parameters under variety of micrometeorological conditions and fixing the best parameters giving lower error in comparison to remote sensing data. Furthermore, validation is achieved by running the calibrated model and comparing the result with the ground data such as measured evapotranspiration from lysimeter and eddy covariance methods.

1.6. Research objectives

1.6.1. General objective

The main goal is to assess the capability of SCOPE model to retrieve the accurate evapotranspiration from airborne hyperspectral data, and to validate the results with the ground data.

1.6.2. Specific objectives

- To conduct sensitivity analysis for investigating the effects of biophysical and biochemical parameters on spectral radiation.
- To evaluate the quality of airborne hyperspectral (AHS) data.
- To retrieve leaf optical properties and canopy structure parameters from optical domain AHS sensor.
- To retrieve biochemical parameters from thermal domain AHS sensor.
- To quantify evapotranspiration for three different land cover.
- To validate the performance of SCOPE model for evapotranspiration with ground data.

1.7. Research questions

- How sensitive is spectral radiation to biophysical and biochemical parameters?
- How can leaf optical properties and canopy structure parameters be estimated from airborne hyperspectral scanner on the reflectance domain?
- How can biochemical parameters be estimated from airborne hyperspectral scanner on the thermal domain?
- How accurate is the SCOPE model for the retrieval of evapotranspiration?

1.8. Innovation of this research

- In this study, quantifying evapotranspiration will be done based on optical and thermal radiation from AHS sensor with the high spectral and spatial resolution while previous studies did not use airborne data (AHS) sensor. Problems resulting from mixed pixels are avoided and additional information from narrow bands is used properly.

- The SCOPE model will be calibrated and validated with ground data where SCOPE model has not been calibrated and validated based on airborne over agriculture area before.

- By using the SCOPE time series model, it has ability to generate fluxes from instantaneous data to daily during the flight overpass.

1.9. Research outline

This thesis is organized in the following manner:

- The first chapter contains background on evapotranspiration and modelling. It also presents research justification, research problem, research question, objectives and innovation of this research.

- The second chapter describes basic theory of SCOPE model.

- The third chapter describes study area in Spain and the datasets used.

- The fourth chapter describes the applied methodology and data analysis.

- The fifth chapter presents the results obtained to achieve objectives.

- The sixth chapter discusses results obtained.

- The seventh chapter provides the conclusion and recommendation.

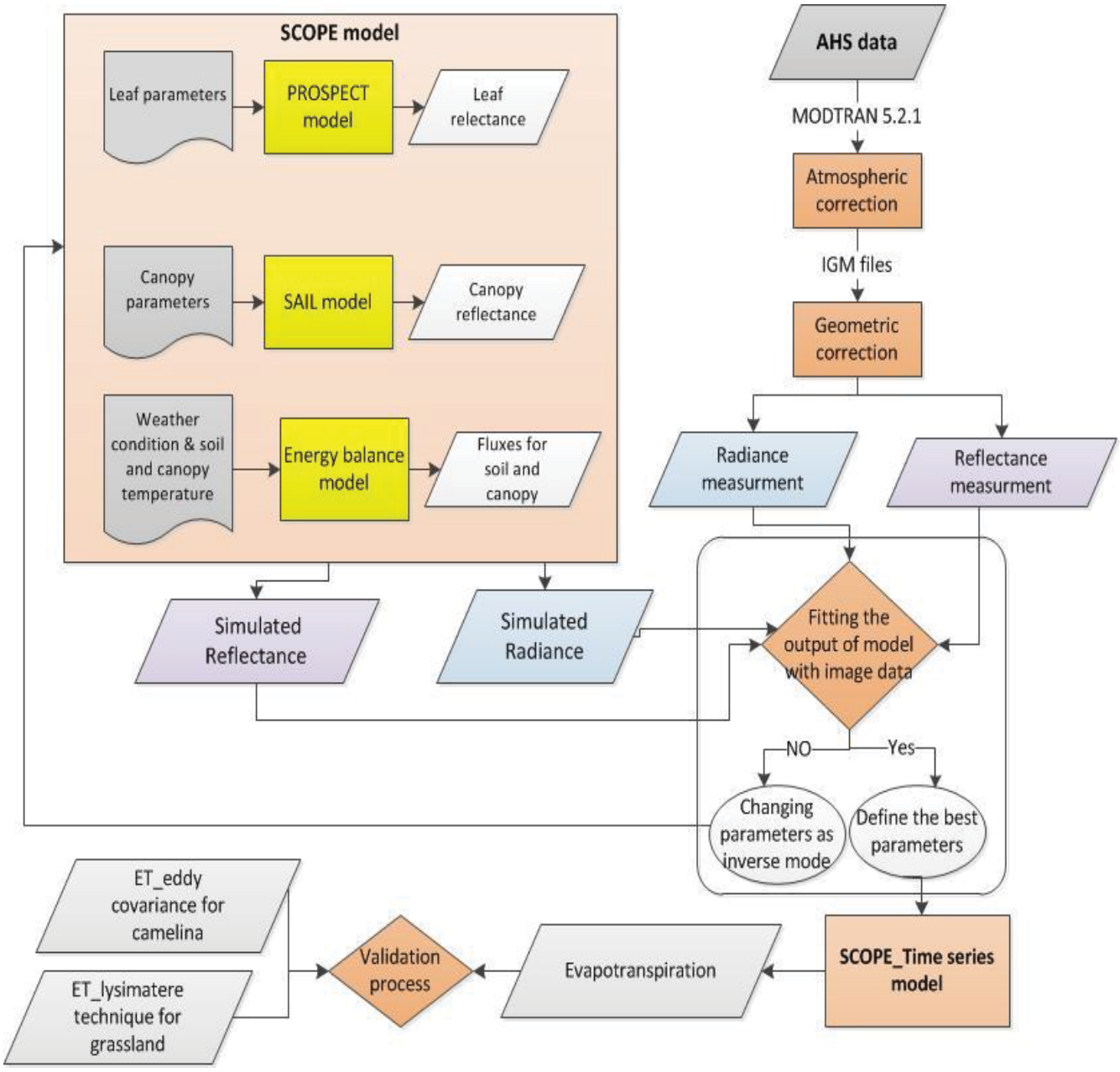

Figure 1-1: Conceptual frame work of this research

2. THEORETICAL BASIC OF THE SCOPE MODEL

This chapter describes the scheme of SCOPE model for simulating fluxes of canopy-atmosphere interaction which was developed by (van der Tol et al., 2009) at the ITC International Institute for Geo-Information Science and Earth Observation in The Netherlands, in the framework the ECO-RTM project, funded by the Netherlands Organization for Scientific Research (NWO-SRON-EO71). All equations related to this model were written in (van der Tol et al., 2009) and written in Matlab script to facilitate using this model.

2.1. Overview of the SCOPE Model

2.1.1. Model structure

The SCOPE model is a biophysical model which can predict the behaviour of the land use system with radiative transfer model and environmental effects (van der Tol et al., 2009). It is 1 D vertical dimension with ignoring variations in the horizontal direction and it is integrated radiative transfer and energy balance model. RTM estimates the TOC spectrum radiation in observation direction and distribution incoming radiation as well as net radiation at surface elements to use it as input of energy balance model. It calculates turbulent heat fluxes, photosynthesis, fluorescence and skin temperature at surface elements to use it as input of radiative transfer model, where output of energy balance model is the input of RTM and so on.

Canopy architecture is an important factor for SCOPE model so that the spatial role of plant morphology specially the leaf inclination, leaf orientation and leaf azimuth angles effects on the pattern of light availability within the canopy. The SCOPE model divides leaves and soil into classes of sunlit and shaded which is receiving different irradiance. It divides the vegetation into 60 layers, 13 leaf inclination classes and 36 leaf azimuth angles with respect to direction of the sun as the one used in SAIL model (Verhoef, 1984).

SCOPE model is built on the basis of linearity of the radiative transfer equation which is combined functions related to the optical, thermal domain and direct solar, sky radiation generated from sunlit and shaded soil and sunlit and shaded leaves. From here SCOPE model can be estimated photosynthesis, chlorophyll fluorescence and energy balance at top of canopy up to atmosphere. It has opportunity to use each module separately or as an integrated unit based on application.

The SCOPE model consists the following:

1. The first module is PROSPECT (Jacquemoud et al., 1990)for estimating optical properties of leaves which depends on the chemical and physical characteristics of leaves.
2. The second module is SAIL (Verhoef, 1984) used for estimating optical properties of canopy based on leaf area index and leaf inclination distribution as well as the optical properties of leaves coupled with measurement conditions.
3. The third one is energy balance module for estimating fluxes based on the heterogeneous of canopy and soil temperature.
4. The last one is FlourSAIL (Miller et al., 2005) module which calculates spectrum radiation of chlorophyll fluorescence from leaves and the canopy architecture based on irradiance, canopy temperature and other environmental conditions but in this research, this module will not use.

The details of each module for the SCOPE model are described as follows:

- RTMo module (transfer of solar and sky radiation)

RTMo is semi analytical radiative model for incident solar and sky radiation based on the SAIL model (Verhoef, 1984) which is one of the oldest models studied the interaction between incoming radiation and leaf canopies after (Suits, 1971)model cooperated with PROSPECT model (Jacquemoud et al., 1990; Jacquemoud et al., 2009).
PROSPECT parameters (N, Cab, Cw, Cm and Cs) and SAIL parameters (LADF (a+b), hot spot, soil reflectance, SKYL, SZA, SAA, RAA and LAI) as well as incoming radiation of solar and sky will be used as input in model. RTMo module estimates the outgoing radiation from 0.4 to 50 μm and net radiation (Rn) to know the amount of radiation absorbed, as well as fraction absorbed photo-synthetically active radiation (fAPAR) for soil and vegetation.

- RTMt module (transfer of radiation emitted by vegetation and soil)

RTMt is a numerical radiative transfer model for thermal part. It depends on thermal radiation generated from different temperature of soil and vegetation. (Verhoef et al., 2007) stated that the soil and vegetation components have different temperatures in the sun and in the shade based on the incoming radiation.
The input parameters of RTMt are the output of energy balance module: the leaf and soil temperature (sunlit/shaded). It is mainly based on iteration process which links between RTMt module and the energy balance module. The output of RTMt used as input of energy balance module is TOC outgoing thermal radiation and net radiation for leaf and soil. This process carried out matching between input variables of the thermal radiative transfer and output of the energy balance module and vice versa.

- Energy balance module

The energy balance module is used the output of RTMo and output of RTMt. In addition, it uses measure weather conditions (air temperature, wind speed, vapour pressure) as input. The output is turbulent heat fluxes, photosynthesis, chlorophyll fluorescence, aerodynamic resistances and skin temperature at surface elements.

- RTMf module (transfer of chlorophyll fluorescence radiation):

RTMf is a radiative transfer for chlorophyll fluorescence based on FluorSAIL model (Miller et al., 2005) The input parameters are chlorophyll fluorescence generated from the energy balance module to estimate TOC outgoing radiation of chlorophyll fluorescence from leaf and the geometry of the canopy. Each Module is complementary to the other. In this research, RTMf module was not used. Modules are organized as order shown in Figure 2-1.

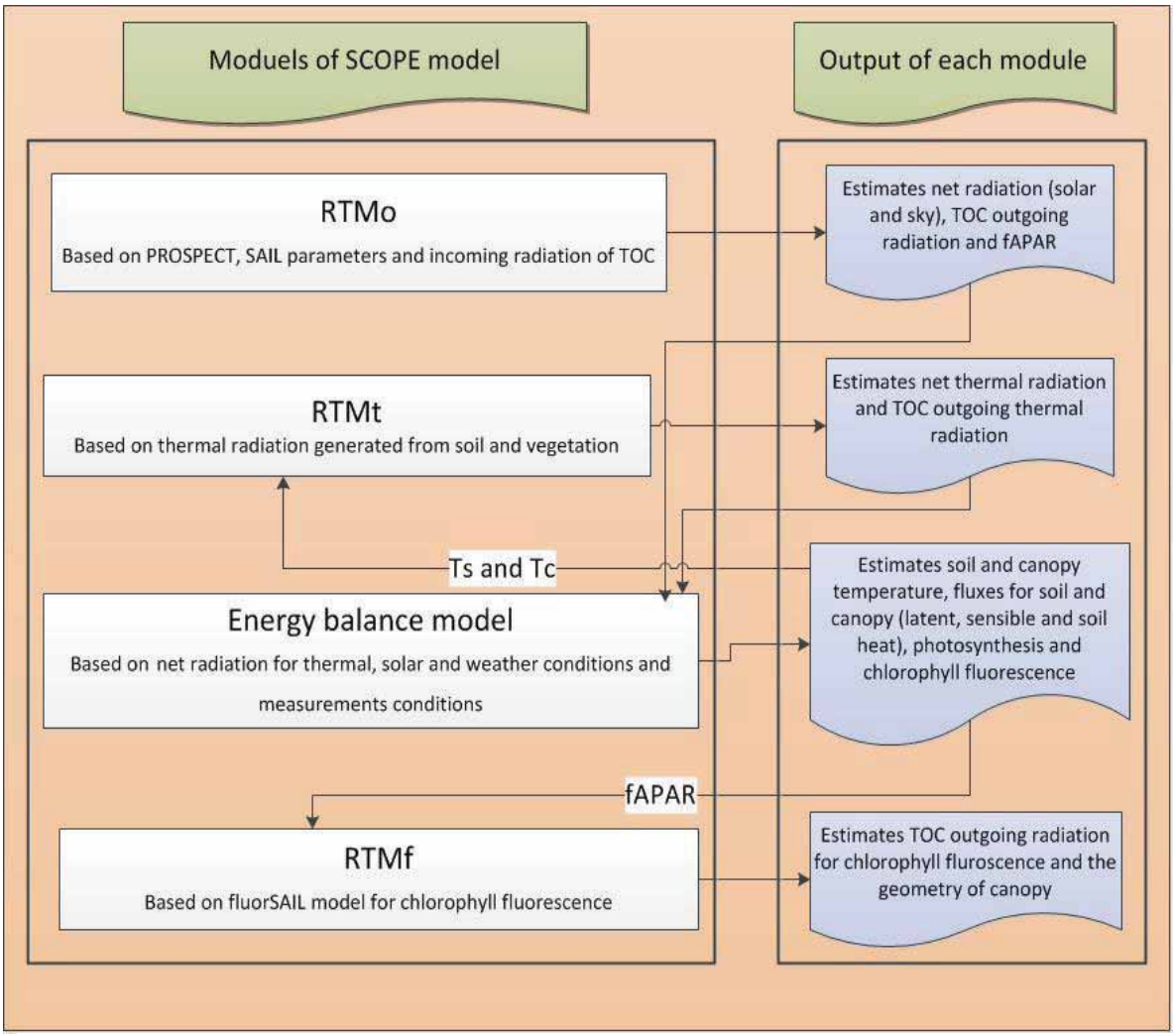

Figure 2-1: Structure of the SCOPE model

2.1.2. SCOPE model dealing with optical and thermal part

SCOPE model version 1.34 has been implemented in Matlab. SCOPE consists of several scripts where each script performs a particular function based on the application (van der Tol et al., 2009). Two types of scripts were used in this study. It is SCOPE.m and SCOPE_TS.m. before running model; it should be decided what the purpose to use it and then specified the input data is required.

2.1.2.1. The optical part of SCOPE model

The SCOPE.m script was used for building look up tables. It has option to run model for optical part only and switch off the other option for thermal part. The LUT approach depends on specified PROSPECT-SAIL parameters organized in a structure in which more than one value can be given to each parameter in the form an array. By running the script, all possible combinations of specified parameters are used to simulate the reflectance. The results saved in a text file. It also has the option to specify the location by defining longitude and latitude. Moreover it is required to specify the weather conditions and canopy geometry (SAZ, SAA and RVA) during the flight overpass. The reflectance generated from model was used to match with the measured data to retrieve the parameters.

2.1.2.2. The thermal part of SCOPE model

By using the same script SCOPE.m, it can be switch on using the 'calcplank' option and 'calcebal' option for simulating full spectrum on thermal range and energy balance along as vertical profiles within canopy. Leaf biochemical parameters, aerodynamic resistances and soil parameters were specified by using LUT. In addition, C3 or C4 vegetation was specified based type of plant. The model runs with all parameters by user to simulate thermal radiation compared with spectrum radiation from image data.

2.1.3. SCOPE time series model

In the SCOPE model, there is another script called SCOPE_TS for time series. It is able to generate fluxes from instantaneous data to daily. The parameters must be specified in script Parameters.m which contains location of input data, leaf- canopy parameters, biochemical parameters, aerodynamic resistance as constant values and weather conditions. Weather conditions are provided as time series.

2.1.4. Output of SCOPE model

2.1.4.1. Spectra radiation

The output of SCOPE is the spectra radiation for the optical and thermal and chlorophyll fluorescence above the canopy. The optical spectrum is reflectance from 0.4 to 2.5 μm based on leaf and canopy properties, whereas the thermal radiation is radiation from 3 to 50 μm based on biochemical parameters and skin temperature of the soil and plant. Soil and plant have different emissivity where emissivity of plant is higher than emissivity of soil. The last radiation is chlorophyll fluorescence spectra in visible bands from 0.6 – 0.85 μm (van der Tol et al., 2009).

2.1.4.2. Directional radiance

By using the SCOPE model, it is possible to study the different viewing angles that affect reflectance, brightness temperature and chlorophyll fluorescence. On the reflectance spectrum, multi-angular observation reveals biophysical and biochemical parameters better than nadir angle. On thermal band, the brightness temperature increases with increasing viewing angle from vertical to horizontal. The last one, the increasing viewing angle from vertical to horizontal will increase chlorophyll fluorescence spectra consequently (van der Tol et al., 2009).

2.1.4.3. Vertical profiles

The bottom leaves (sunlit and shaded) have different temperatures than top leaves. Sparse vegetation usually has higher temperatures than dense vegetation with a high leaf area index. The different temperatures result from incoming radiation, weather conditions affecting the energy balance and the turbulent heat fluxes (van der Tol et al., 2009).

3. STUDY AREA AND AVAILABLE DATA

3.1. General description for study area

The research was done within the Castilla-La Mancha region Barrax, Spain which is agricultural land at 700 m above sea level. It is flat landscape and the experimental farm ' Las Tiesas' belong to the " Escuela Te'cnica Superior de Ingenieros Agronomos" of the University of Castilla- La Mancha (Timmermans et al., 2012). Within this region, the test site La Tiesas farm is located between Barrax and Albacete province with coordinate 39^{o} 14' 45'' North, 2^{o} 5' 1'' West 20km away from the capital town Albacete (Timmermans et al., 2012). Total area is approximately 5*6 km^{2}. Many studies have been carried out in the Las Tiesas experimental farm, operated by ITAP, including previous campaigns for calibration and validation of remote sensing observations to study biophysical vegetation processes (Sobrino J. A. et al., 2008; Su et al., 2008).

The Mediterranean climate is characterized in this region which is dry in summer and winter. It is rainy in spring and autumn with potential evapotranspiration is of 5 mm/d and annual rainfall of 400 mm (Shifa, 2011). In this region, it has regional ground water table about 20-30 m below the land surface (Timmermans, 2011).

The landscape area presents different types of soil: the most common is Petrocalcic Calcixerepts which is suitable for agriculture (Timmermans, 2011). This area is cultivated by vineyard and irrigated plants corn, barley, sunflower, poppy, forest nursery, grass and camelina at Barrax test site. During airborne overpass, the camelina was senescent but corn and grass was maturity stage.

3.2. Description of the REFLEX campagin

The research was carried out under the REFLEX framework (Regional Experiments for Land-atmosphere Exchanges) during 18-28 July 2012 which is funded by a grant awarded by EUFAR(EC FP7) organized an International Conference on Airborne Research for the Environment in Toulouse. REFLEX campaign had the following objectives (Timmermans et al., 2012):

- To assess image products over the land.
- To understand the links between radiative transfer model and an energy balance in land-atmosphere interaction by using AHS and CASI sensors.
- To validate of biophysical and biochemical parameters derived from satellite data and airborne hyperspectral with ground data.
- To provide acquisition of simultaneous multi-temporal, multi-angular and multi-sensor hyper-spectral data over a heterogeneous area.
- To simulate soil moisture with high accuracy by using multi-angular optical and thermal observations.

This study aims at achieving the first and second of these REFLEX objectives, which provided and supported the airborne data processing and analysis.

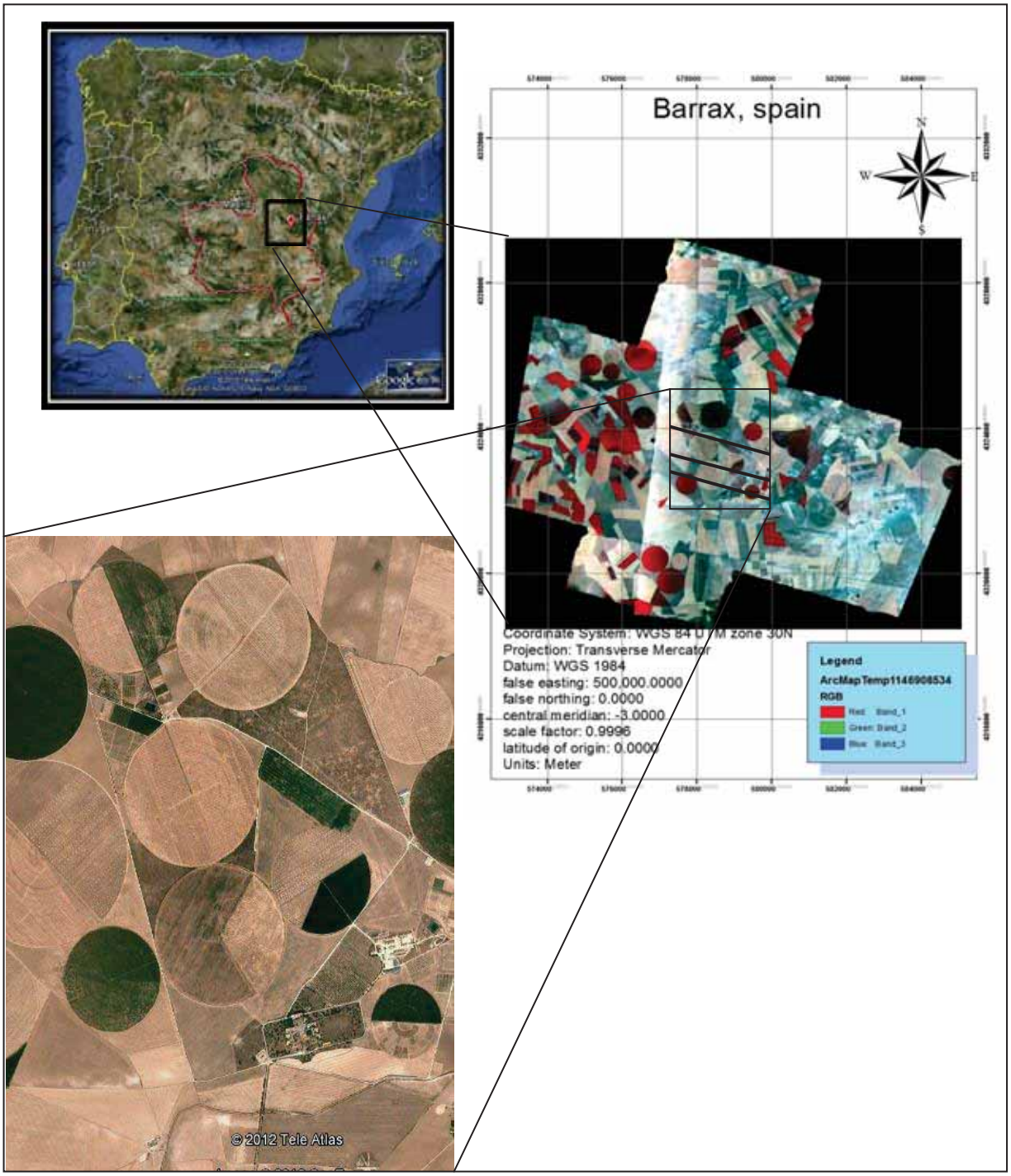

Figure 3-1: (on the left) it is whole area of Spain, (on the right) it is mosaic of AHS data covered by flight tracks and the last figure (on the left) La Tiesas farm in Barrax, Spain provided by REFLEX campaign.

3.3. AHS Data acquisition

During REFLEX campaign, CASA 212-INTA airplane was used for mounting the AHS and CASI sensors to acquire valuable data for bio-geophysical parameter estimation (Timmermans et al., 2012). In addition, ASD and Everest radiometers were used for measuring reflectance and emission from calibration targets in the solar and thermal range of the electromagnetic spectrum but these data hadn't been processed and delivered in time for this research. Airborne hyperspectral data was available and required in this study to detect physical condition of vegetation and bio-geophysical parameter retrieval from optical and thermal. They were used also to test the performance of the SCOPE model.

3.3.1. Imagery acquired

The AHS flights took place on 2 days: 25h of July 2012 (flight 1) and 26th of July 2012 (flight 2). Flight started at (08:41) UTC and finished at (09:47) UTC. And on the same day at night (21:01-21:40 UTC) flight took place (flight 3). It was composed by 20 images acquired at (low altitude) 1000 m above ground level for first day and second day at (high altitude) 2000 m above ground level.
The first day of images (25th of July 2012) is used because it was already calibrated but the second day's data weren't available yet during this study. The flight took five lines to cover study area referred to as P01, P02, P03, P22N and P21N. Each line track has true heading. But for this study, the track P03 was selected with 287º, afterward P03 (W-E) is repeated with opposite heading (107º). This repetition is referring to avoid variable wind at altitude above terrain 1859 m.

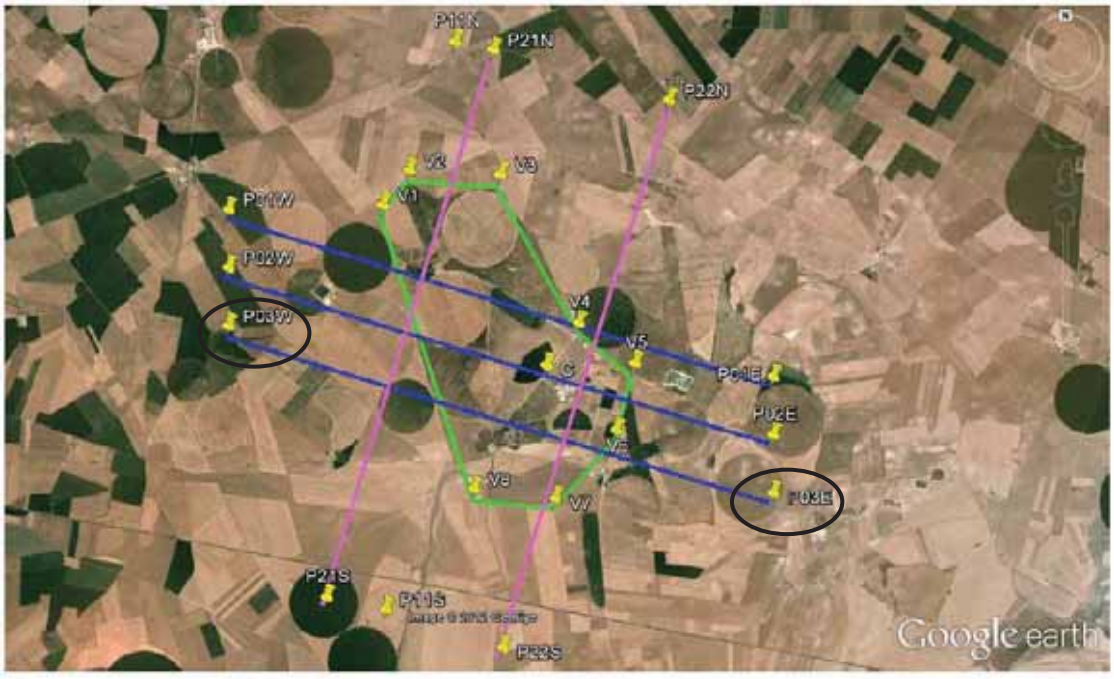

Figure 3-2: EUFAR, REFLEX 2012 AHS flight tracks P01, P02, P03, P22N and P21N. The last track P03W-E was used for analysis "Las Tiesas" test site, Barrax, Albecete, Spain at MSL(mean sea level)900FT(foot feet) provided by REFLEX campaign

3.3.2. AHS-INTA Technical characteristics

During the REFLEX campaign, the AHS (airborne hyper-spectral scanner) (developed by SensTech Inc., currently AgronST, USA) was organized with in-situ measurements. It was placed on board the INTA's (Spanish Institute of Aeronaoutics) aircraft CASA 212-200 Paternina (EADS). The AHS is line scanner and it has 80 spectral bands including 63 bands in the reflective part of the electromagnetic spectrum, 7 bands in the 3 to 5 micron range and 10 bands in the 8 to 13 micron region. 'The first element of the system is a rotating mirror which directs the surface radiation to a cassegrain-type telescope. The telescope design includes a so called pfund assembly, with field of view (FOV) around 90° (± 45°), the instantaneous FOV is 2.5 mrad, the ground FOV is 2–6 m at 140 kt cruise speed; scan speed: 6.25, 12.5, 18.75, 25, 31.25, 35 rps; 12bits digitized; 750 samples per line, an AHS pixel subtends 0.12 degrees and minimum pixel size is 2 m for spatial resolution (Sobrino et al., 2006)'. In the spectrometer, four diachronic filters are used to split the incoming radiation in five optical ports: (VNIR), single band at 1.6 micrometer, (SWIR), (MIR) and (TIR) (Timmermans et al., 2012).

Table 3-1: Main characteristic of airborne hyperspectral scanner (AHS)

Information of ports	PORT 1	PORT 2A	PORT 2	PORT 3	PORT 4
Coverage (nm)	443-1019	1491-1650	2024-2498	3030-5410	7950-13700
Bandwidth (FWHM)	27-30 nm	159 nm	12-13 nm	260-420 nm	400-550 nm
N $\Delta\lambda$ (minimum)	17	10	156	9	17
Number of bands	20	1	42	7	10

3.3.3. AHS data products and quality of images

The AHS file has 2 levels L1 and L2. Level 1 includes 3 products (L1a, L1b and L1c) and Level 2 includes 2 products (L2b and L2c). The flight organization performed some processing of the images. They did calibration for raw data (L1a) but L1c and L2c products hadn't been completed. Table 3-2 shows the details of each type of products. In level 2b, reflectance, temperature and emissivity have been computed with ATCOR4. Closer inspection of the data showed that the values were selected for doing atmospheric correction such as visibility, water vapour and aerosol type appeared not realistic values of the actual atmospheric conditions. Table 3-2 explains the characters of image products.

Table 3-2: AHS data product

Level image product	Raw product L1a (L0R00)	Image product with 80 bands in BIL format + ENVI header and ancillary information.
	L1b product (L10020/L00120)	It contains: - Images calibrated at sensor radiance (nW/cm^2 sr nm) with BSQ format. Reflective bands (1-63). Thermal band (64-80). - Image geometry map (IGM) files have two layers (x and y coordinate). - Metadata includes sensor height above ground, zenith angle and azimuth angle.
	L1c product (L10022/L00122)	It is georeferenced calibrated at sensor radiance only three bands for reflective bands and one band for thermal bands.
Level image product	L2b product (L20020/L20120)	It contains - AHS hemispherical directional reflectance retrieved by ACTOR4 per %*100. - Surface temperature estimated by ACTOR4 per Celsius*100. - Surface emissivity estimated by ACTOR4 per %*100. - Image geometry map (IGM) files the same as L1b. - Metadata the same as L1b.
	L2c product (L20022/L20122)	It is georeferenced L2b products.

3.4. Micrometeorological data and ground measurements

The ground data used in this study were provided under the REFLEX campaign by a team of the University of Twente, Politecnico de Milano and CEAM. They measured boundary layer heat and moisture fluxes above the canopy as well as above bare soil. And also they measured meteorological variables from 16th to 28th July 2012. (Timmermans et al., 2012) state that three flux towers were installed one over the camelina, one over the vineyard and another over the reforestation area. In addition a Large Aperture Scintillometer was installed over wheat stubble field. Furthermore an ITAP operated lysimeter station at the vineyard site and grass site records actual evapotranspiration and soil moisture as well as standard meteorological measurements at 2 m which are stored on an hourly basis. In this research, flux tower over camelina and lysimeter station over grass were used for validation of model results.

3.4.1. Micrometeorological data

Flux tower observation at camelina site with coordinate 39°02'30.84" N, 2°04'56.7" W (WGS84) and lysimeter station at the grass site with coordinate 39°03'35.15" N, 2°06'33.66" W (WGS84) recorded meteorological data. Meteorological information was necessary to use it as input in SCOPE model. On EC tower a variety of instruments and sensors was installed from 16th to 29th July 2012 for measuring weather condition with different altitude and pre-processing data was implemented by REFLEX campaign.

Table 3-3: The instruments and sensors of eddy covariance tower

Model	sensor	Data measurement
HOBO	Soil heat sensors	Soil temperature
Degacon SN: EM7168	Soil moisture sensor	Soil moisture at depth 5, 10 and 20 cm
Campbell Sci. CS215	RTH sensors	Relative humidity (RH), air temperature (Ta) at (1.3, 2.10 and 4.1 m above surface).
Hukseflux HMP1	Soil heat flux plates	Ground heat flux at depth (8 and 13 cm)
LICOR L1 7500 (Lico Inc,USA)	CO_2/H_2O infrared gas analyzer	The fluxes from land surface at 2.38m above surface.
GILL 2D and CSAT3	Sonic anemometers	Air pressure (P), wind speed (u) at (1.3, 2.38 and 5.20) m above surface
CNR 1 (Kipp and Zonen, SN: 071358)	Radiometer	Shortwave incoming and outgoing (Rsi, Rso), Longwave incoming and outgoing (Rli, Rlo) at 1.0m height.

These Flux data and weather data are available at 30 minutes intervals, at 10 minute interval, at 1 minute interval and at 10 second interval except for wind speed and direction at 5.2 m. Airborne flight passed on 207.40 DOY so the weather condition was specified from file at 10 sec interval into SCOPE model. For estimating ET daily, the file at 30 minutes was used with height 4.2 m.

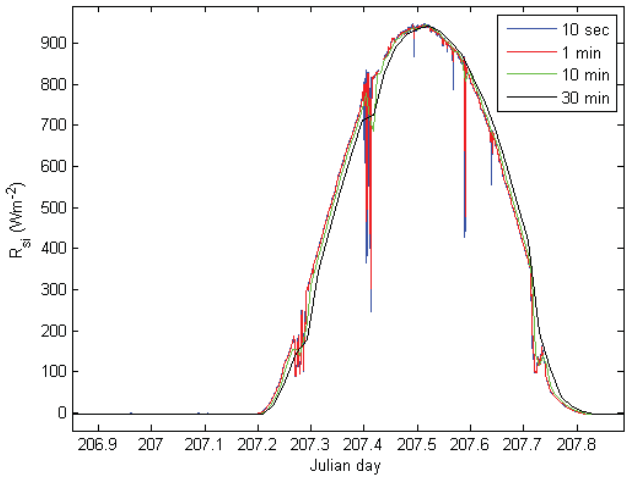

Figure 3-3: Incoming radiation short wave of EC tower over camelina site (Source: Timmermans et al., 2012).

At grass site, the data is recorded over 60 minute's interval under supervisor Juan-Carlos Jimenez-Munoz. The field data measured net radiation above the canopy, as well as wind speed (m s^{-1}) vertically, air temperature(°C), the water vapour density and CO_2/ O_2 density (mg m^{-3}). In addition, relative humidity, air temperature at height 2 m, air pressure (hPa), soil moisture at 10 and 40 cm depth, soil temperature and the four component radiation were measured. Data started measurement on the 23th and continued until 30th July 2012.

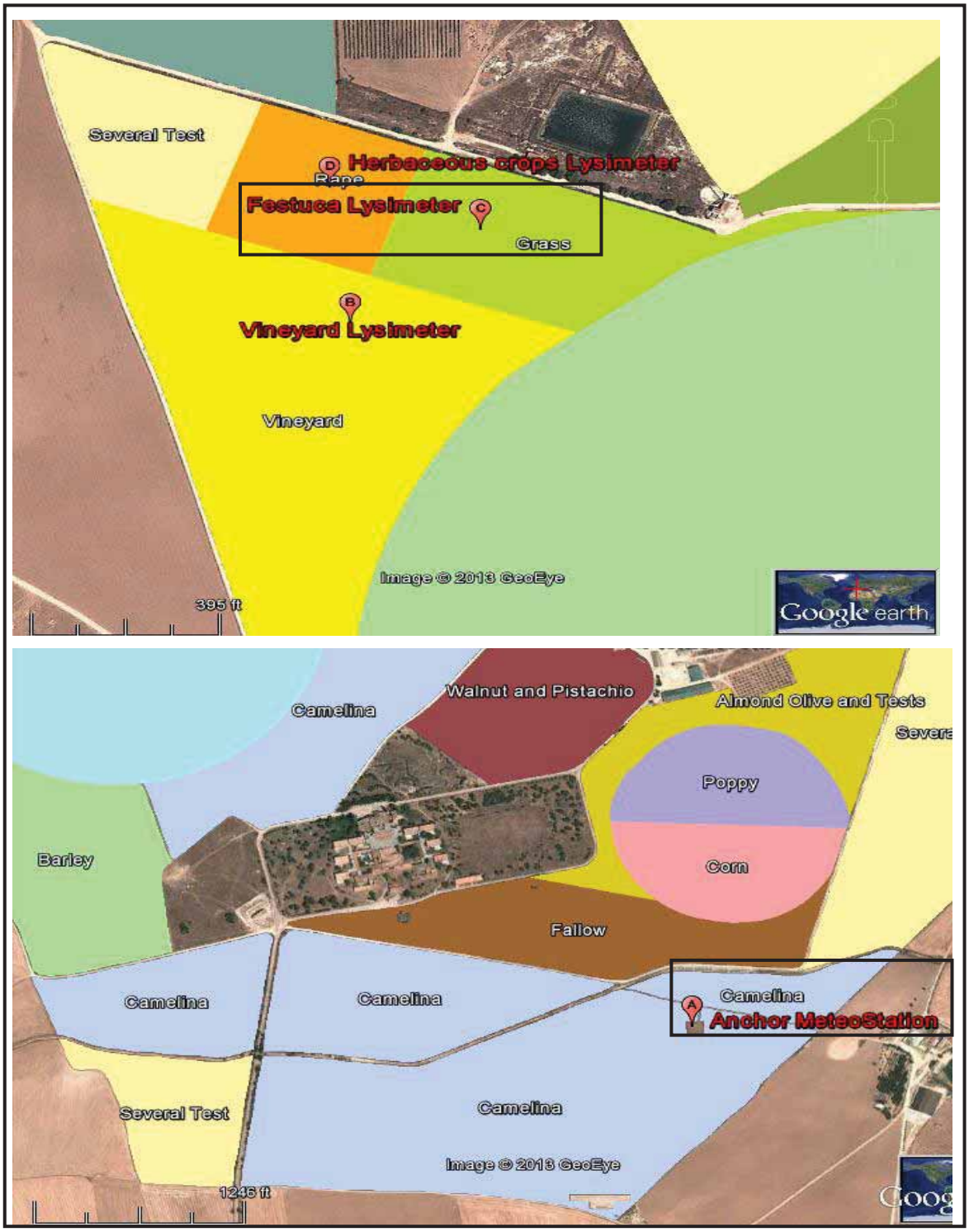

Figure 3-4: The upper map shows the location of lysimeter station for grass and the lower map shows the location of EC flux tower for camelina provided by REFLEX campaign

3.4.2. Ground measurements

Measurements of boundary layer heat and moisture fluxes provided by field campaigns which play big role for testing SCOPE model by validation process for ET from aircraft. During REFLEX campaign operated by ITAP, the flux tower was installed from 16th to 29th July 2012 at the camelina site with flux measurements at 1.3, 2.4 and 4.1 m height in Figure 3-5. For grass, The Festuca lysimeter technique was installed from 23th to 30th July 2012 to calculate ET daily in Figure 3-6.

Figure 3-5: Eddy covariance flux tower at the camelina site

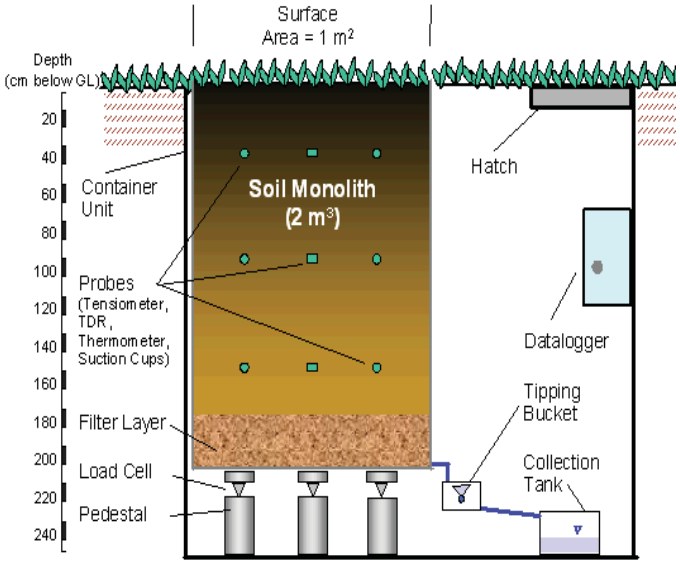

Figure 3-6: Festuca lysimeter technique for grass

4. METHODOLOGY

4.1. Method overview

The following processing steps were undertaken:

1. Atmospheric and geometric corrections (Figure 4-1).
2. Selecting pixels representing the three types of canopy: corn, camelina and grass.
3. Model inversion procedure to estimate PROSPECT-SAIL parameters by building LUT from the optical domain of AHS data.
4. Model inversion procedure to estimate biochemical parameters by building LUT from the thermal domain of AHS data (after fixing PROSPECT-SAIL parameters with step 3).
5. Forward modeling to quantify evapotranspiration for the three canopy types within the selected pixels.
6. Generating time series of evapotranspiration for grass and camelina (for corn, meteorological and validation data were not present).
7. Validation process by comparison between ET simulated from SCOPE model and ET obtained from eddy covariance measurements and lysimeter technique for camelina (*C. sativa* L.) and grassland respectively.

❖ The description of each step of the methodology is preceded by a simple flowchart.

Step 1: preparation of the AHS data

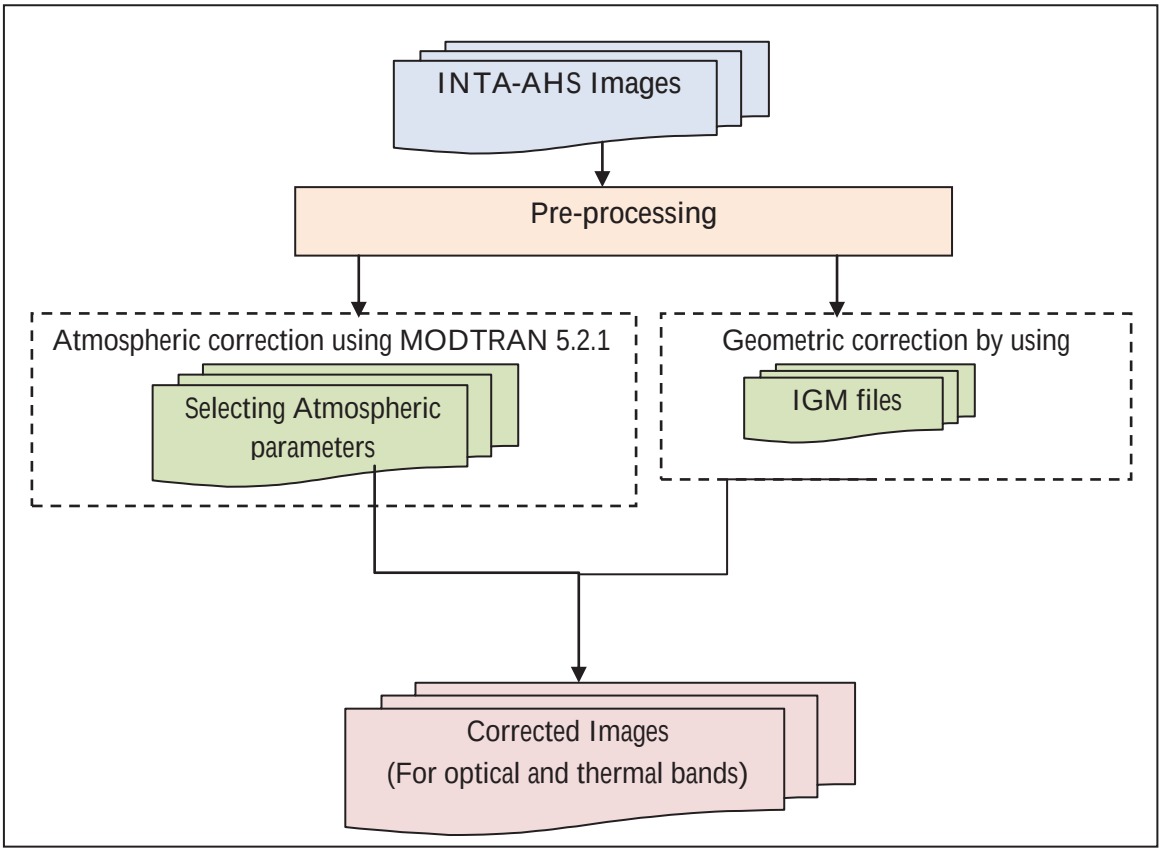

Figure 4-1: Overview pre-processing AHS data

4.2. Pre-processing of AHS data:

4.2.1. Atmospheric correction

Atmospheric correction is the most important part of the pre-processing where the AHS airborne data has to be atmospherically corrected (AC) to achieve full spectral information from pixels. The level 2b products included surface reflectance and surface temperature (correcting using band 75) and surface emissivity were corrected by using ATCOR4. However, the corrected needed improvement because it was not carried out for the actual atmospheric condition during the airplane overpasses (Timmermans et al., 2012).

Atmospheric corrections of AHS data were performed by using MODTRAN 5.2.1 based on radiative transfer equation. It was developed by AFRL/NRL in collaboration with Spectral Sciences, Inc. The MODTRAN code was written in Matlab script to calculate atmospheric transmittance and radiance with high spectral resolution 0.1cm^{-1}. The input file of MODTRAN is called 'tap5' and contains specific parameters to define the real condition as shown in Table 4-1. The output file is called tap7. The visibility is the most sensitive parameter for input MODTRAN 5.2.1. The values of water vapour (g/cm^2) and AOT (unit less quantity) are directly influencing the visibility.

Measured value for visibility was not available. Figure 4-2 shows that the changing visibility parameter directly affects reflectance so that producing a LUT for visibility is required to estimate realistic value for the specific case of the campaign in Barrax, Spain. Fig 4-2 clearly shows that the peak change is caused by the variation of visibility. In visible band from 0.4-0.7 μm, the peak of the reflectance will increase gradually with increasing visibility values. The visibility was used for which, no negative reflectance and close to zero. This step was required to obtain ascertain surface reflectance from AHS data.

Table 4-1: The input parameters of MODTRAN 5. 2. 1

Input parameters	Values
Geographical-seasonal model	Mid-latitude summer (45^o north latitude)
Concentration of carbon dioxide (ppm)	385.000
Water vapour (g/cm^2)	0.4
Ozone (ppm)	0.000
Visibility(km)	20, 25,30, 35, 40, 45, 50, 55,60 (LUTs)
Surface temperature (K)	0.001
Albedo	0.00, 0.50, 1.00
Surface height (km)	0.70000
Sensor height (km)	2.734
Relative azimuth angle (degree)	89.20
Solar zenith angle (degree)	40.9
Start, end wavelength ,increment and band width (nm)	400-2500 nm, 1.0, 1.0 (optical part) 8310-12950.0 nm, 20.0, 20.0 (thermal part)

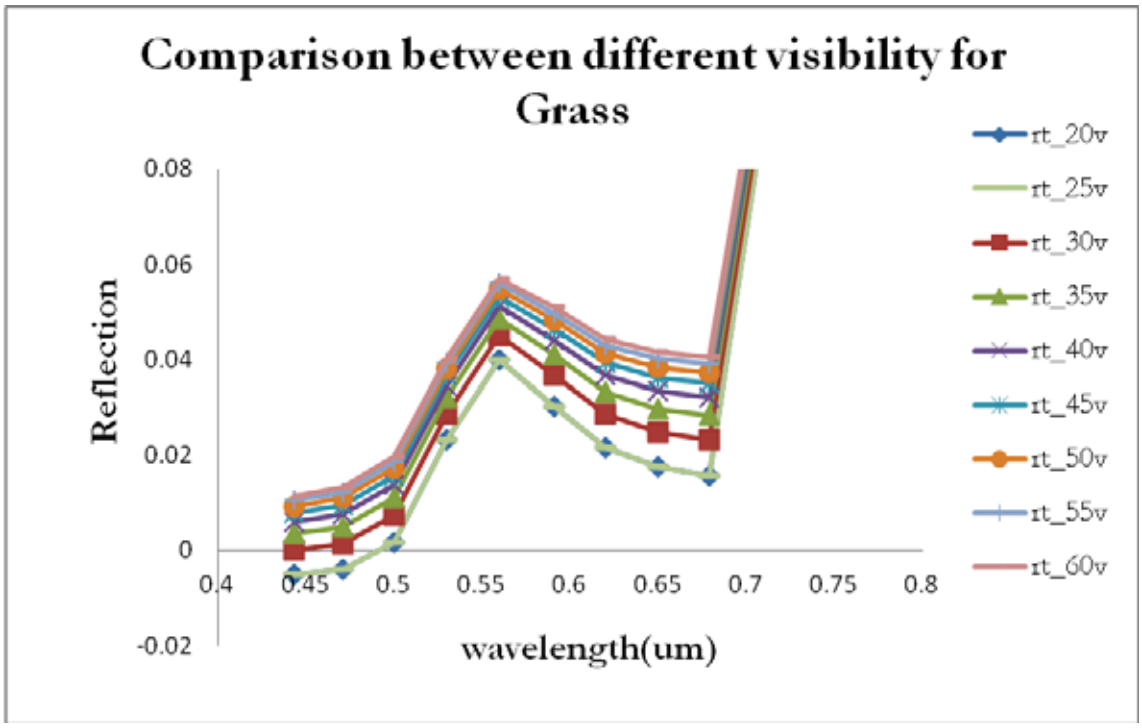

Figure 4-2: The effete of changing visibility on the reflectance in visible bands

4.2.1.1. Atmospheric corrections of airborne optical remote sensing data

(Yuanliu et al., 2008) stated that the radiance from target region is mainly effected by three constitutes: 1) radiance scattered by atmosphere in to viewing direction, 2) radiance reflected from the target and transmitted in to the viewing direction, 3) radiance reflected from the background which is called adjacent effect. In order to retrieve radiance from the target observed by sensor, the surface is assumed uniform and has Lambert reflectance. The radiance measured by the sensor on the board of the aircraft can be written as follows (Verhoef, 2012).

$$L = L_0 + \frac{G_t r_t + G_b r_b}{1 - r_b S} \quad \text{.....1}$$

where L (mW/cm² sr nm) is radiance measured by sensor, L_0 (mW/cm² sr μm) is the atmospheric path radiance for black earth's surface, G_t is the gain factor of target, G_b is the gain factor of background, r_t is the target pixel reflectance, r_b is the background reflectance from surrounding areas and S is spherical albedo of the atmosphere at ground level.

In order to determine all these variables for a given atmospheric condition and observation angles, three times MODTRAN runs should be carried with three surface albedo 0%, 50% and 100% respectively. The output of MODTRAN contains values of frequency, PATH (total path radiance) (mW/cm² sr μm), GRFL (radiance contribution due to ground reflectance sunlight) (mW/cm² sr μm), TOT (total ground reflectance radiance contribution) (mW/cm² sr μm) and the extraterrestrial spectral solar irradiance (Yuanliu et al., 2008). PATH results were obtained from three surface albedo. It is called $PATH_0$, $PATH_{50}$ and $PATH_{100}$. And for GRFL, the output for 50% and 100% were used for calculating reflectance from the target.

For zero albedo, radiance of atmosphere backscattering will be obtained directly from $PATH_0$

$$L_0 = \mathrm{PATH}_0 \quad \text{.....2}$$

For the albedo 50% and 100%, G_t and G_b will be estimated from $GRFL_{50}$ and $GRFL_{100}$ as follow:

$$G_t = \frac{GRFL_{50} * GRFL_{100}}{GRFL_{100} - GRFL_{50}} \quad \text{.....3}$$

$$G_b = \frac{GRFL_{50} * PATH_{100} - PATH_0}{GRFL_{100} - GRFL_{50}} \quad \text{.....4}$$

The spherical albedo of atmosphere at ground can be estimated by

$$S = \frac{GRFL_{100} - 2 * GRFL_{50}}{GRFL_{100} - GRFL_{50}} \quad \text{.....5}$$

All these equations were written in Matlab script and the results of running MODTRAN code is shown in Figure 4-3.

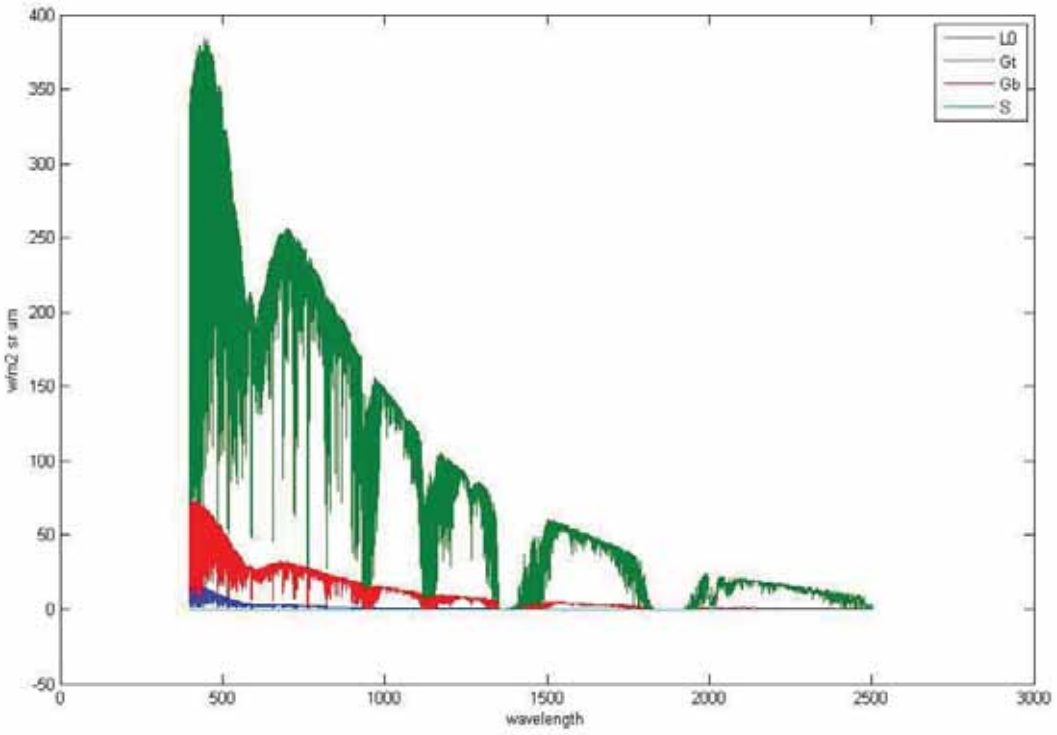

Figure 4-3: The atmospheric parameters (path radiance, gain of target, gain of background and spherical alpedo)

Finally, all the atmospheric parameters were determined. By using Equations 2, 3, 4 and 5, the pixel surface reflectance will be estimated in a simplified form as follow

$$r_t = \frac{L - L_0 + G_b / G_t (L - \bar{L})}{G_t + G_b + (L - L_0) S} \quad \text{.....6}$$

where r_t is the target pixel reflectance, $\bar{L}$ (mW/cm² sr nm)is spatially averaged radiance image which performed by using statistics of ENVI software.

4.2.1.2. Atmospheric corrections of airborne thermal remote sensing data

For thermal domain 3 to 50 μm , the radiative energy emitted from the earth interacts with atmosphere including absorption and reemission by gases. These gases are water vapour, carbon dioxide, ozone and other aerosols. Water vapour has the significant effect on the absorbance incoming radiation for these

wavelengths as well as O_3 and CO_2 are influence atmospheric transmittance. '(Sobrino et al., 2006) found that bands from 71 to 80; thermal range of 8 to 13 μm ; are more effected by noise whereas band 75 (10 μm) shows the highest atmospheric transmittance and band 74 was located in the region of the ozone absorption. However in the AHS flights the ozone observation is not shown because the maximum absorption of ozone is usually located at atmospheric altitudes higher than 10 km'.
Based on this, in order to obtain the surface radiance, changes in the thermal wavelength were conducted in MODTRAN by using the same input parameters for optical part.

Assuming that the surface is heterogeneous and it has non-Lambert radiance from the surface, the radiance measured by AHS sensor can be written as follows (Verhoef, 2012):

$$L = La(t) + \varepsilon Ls\tau_{00} + La(b)(1-\varepsilon)\tau_{00} \quad \text{.....7}$$

where L (mW/cm² sr nm) is the total radiance at sensor height, $La(t)$ (mW/cm² sr μm) is the total top of atmosphere radiance, ε is the emissivity from the surface, Ls (mW/cm² sr μm) is the surface radiance, τ_{00} is direct target sensor transmittance, $La(b)$ (mW/cm² sr μm) is the bottom of atmosphere from surface and $(1-\varepsilon)$ is the reflectance from the target.

For retrieving all these parameters, it is required to run MODTRAN with 0% and 100% surface albedo. PTEM is path thermal instead of PATH. $PTEM_0$ is for surface albedo 0% and $GRFL_{100}$ is required for surface albedo 100%. TRAN is the direct ground-sensor transmittance for the TOA also required.

For zero albedo, radiance from top of atmosphere can be obtained directly by the following equation:

$$La(t) = \mathrm{PTEM}_0 \quad \text{.....8}$$

For the albedo 100%, radiance from bottom of atmosphere can be estimated by

$$La(b) = \mathrm{GRFL}_{100}/\mathrm{TRAN} \quad \text{.....9}$$

The Radiance from the target can be estimated by

$$Ls = \frac{\frac{L - La(t)}{\tau_{00}} - (1-\varepsilon)La(b)}{\varepsilon} \quad \text{.....10}$$

In this study, ε was estimated from prior information for grass, corn and camelina. For grass and Corn, value of 0.98 was adopted (Zhou et al., 2011) and 0.91 for camelina, a dry plant (Olioso et al., 2007).

4.2.2. Geometric correction

After completing atmospheric correction, geometric correction has been performed on the airborne data. Geometric correction is required to avoid distortions caused by instability of the aircraft. The georeference of AHS images was carried out by using IGM file. It contains the x and y map coordinates for each pixel under a specific map projection. The coordinate system was used UTM with WGS84 datum, Zone 30N.

Step2: Inversion SCOPE model for optical domain

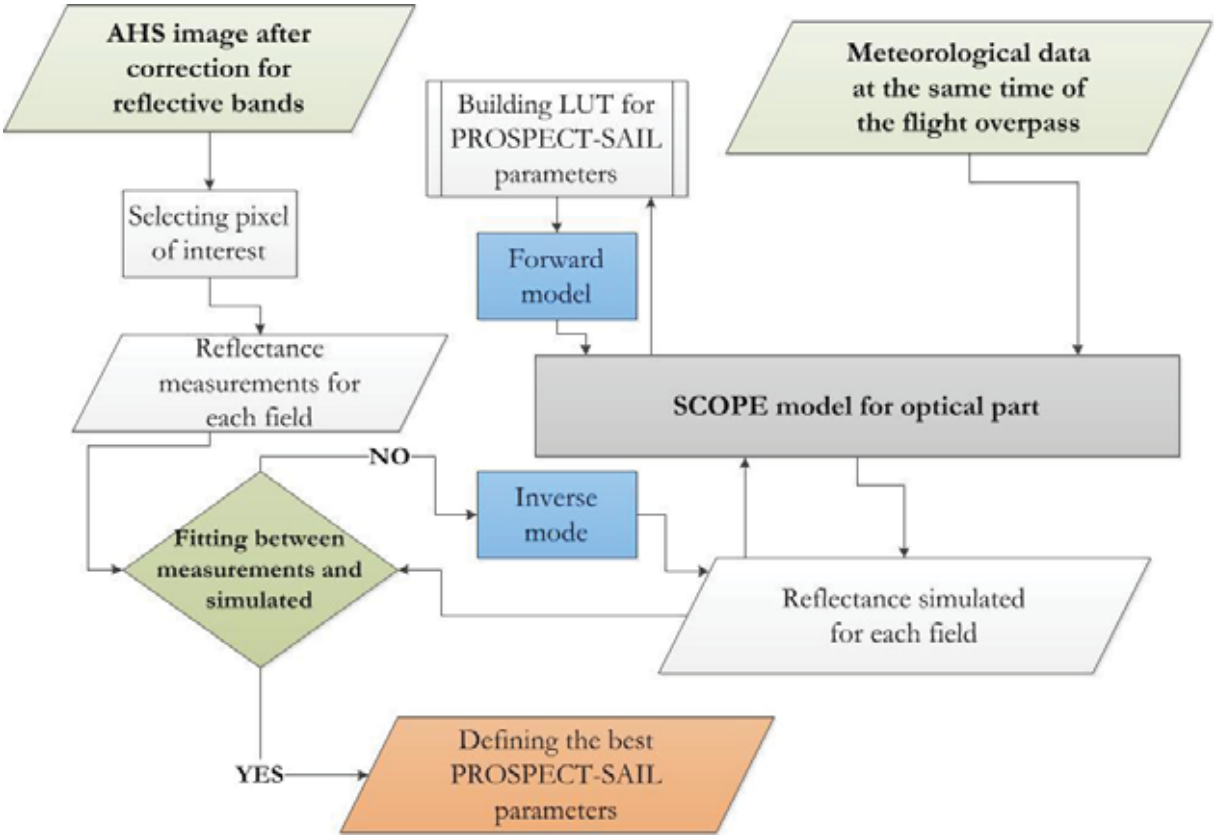

Figure 4-4: Schema of the first part of the methodology (optical part)

4.3. Selection pixel site

The accurately identification of land cover types is critical step for estimating ET into SCOPE model. In order to study the variability of ET over agriculture area, grass, corn, and camelina crops were selected. Camelina is an oil seed crop and has low ET because it was in the senescence stage during AHS flight overpasses comparing to grass and Corn. The determination of ET is required for monitoring crop water requirement.

For some crops such as vineyard, SCOPE model doesn't work well. The reason is that vineyard grows in the form of rows. The structure of the crop violates the assumption of heterogeneity in horizontal direction in the SCOPE model. It is also not built to run for the whole image so that one pixel is enough to calculate ET value for each vegetation cover. Each of these plants has economic importance therefore; the improvement of these plants will increase the agricultural and animal wealth of the country. The next subsections explained each type of plant under study and its importance.

4.3.1. Camelina (*C. sativa L.)*

Camelina (*C. sativa L)* (flax) is an oil seed crop which commonly grows in Europe. The scientific name is *Camelina sativa* (L.) and it belongs to the family Brassicaceae. This crop has high potential for different uses. It has several uses such as livestock feed and bio fuel. It is drought and heat tolerant so that it can grow in arid lands and it needs low requirements of water and nitrogen. Various studies concluded that camelina daily evapotranspiration ranges from 2.0 to 6.5 mmd^{-1} under normal condition over its growing season (French et al., 2009). However, this research has been performed over the region Las Tiesas farm and the crop was almost dry as shown in Figure 4-5.

Figure 4-5: Camelina (*C.sativa L.*), Las Tiesas farm, Barrax, Spain (Source: Timmermans et al., 2012)

4.3.2. Grass

In general, grass is very important for feeding farm animals and it has highly impact on the hydrological cycle due to its high ET so that studying ET process is necessary to understand and estimate the amount of water losses accurately. Based on the growth period and type of fixed carbon, grass can be classified as annual and perennial or C3 and C4 species respectively (Aires et al., 2008). The annual; C3; grass named as Poaceae is one of the canopies under study since it was grown in the research location. It has ability to grow under any conditions such as hot, dry and wet areas.

Figure 4-6: Poaceae Grass, Las Tiesas farm, Barrax, Spain (Source: Timmermans et al., 2012)

4.3.3. Corn (*Z. mays L.*)

Corn is ranked as the third produced food crop in the world (Young et al., 2000). It is cereal crop which belongs to the family Gramineae and Genus *Zea.* It is a C4 plant. In addition, it is most sensitive to drought so it needs high amount of water and it shows daily ET rate exceeding 12 mm d^{-1}(Howell et al., 1997).

Figure 4-7: Corn (*Zea.mays L.*), Las Tiesas farm, Barrax, Spain (Source: Timmermans et al., 2012)

4.4. Forward SCOPE model for optical domain

SCOPE model is a flexible model and covers the spectral range from 0.4 to 2.5 μm. The potential of SCOPE model can be used for the optical part only with ignoring the thermal part and vice versa. At a first stage only, SCOPE model on the optical part was used as a forward mode to determine PROSPECT-SAIL parameters by using LUTs. In the second stage, other LUTs are built for biochemical parameters after fixing PROSPECT-SAIL parameters on the thermal part. The best parameters are retrieved by matching AHS measurements with simulated spectra generated by LUTs. If the spectral information doesn't match, it must be required to tune the input parameters.

Before building the LUT, the sensitivity analysis of the model was analyzed in order to get understanding of the best ranges input parameters for each field.

4.4.1. Sensitivity analysis for optical domain

Sensitivity analysis was implemented to analyze the influence of each parameter on the simulated reflectance during calibration of model where the input parameters control the reflectance response (Jacquemoud et al., 1990). The optical properties of plant leaves started from 0.4 μm to 2.5 μm was used for retrieval the PROSPECT-SAIL parameters. Each plant has a different physiological condition and geometry affecting the reflectance spectra.

By using sensitivity analysis, it can be expected the most dominated ones on the reflectance. The spectral information is divided into three parts. The visible part (0.4-0.7 μm) describes strong absorption of photosynthesis pigments such as Cab, The NIR part (0.7-1.1 μm) is sensitive for N, Cs and LAI refer to the internal leaf structure based on multiple scattering within the leaf. The last part SWIR (1.1-2.5 μm) is more sensitive for Cw than Cdm of leaf and LAI.

4.4.2. Generation LUTs for optical domain

LUTs were implemented as one of the inversion algorithms for testing three types of plants. Each case; camelina, grass and Corn; has different height, VZA and different physiological status during the flight overpass as well as different weather conditions under specific time and day. To run the SCOPE model, the PROSPECT-SAIL parameters was determined by range with a regular step. This range was performed based on the sensitivity analysis for the different land cover units. The other parameters such as canopy geometry and weather conditions remain unchanged as presented in Table 4-3, 4-4 and 4-5. The size of LUTs depends on the range number of parameters. From running SCOPE model, the simulated reflectance was generated from LUTs.

4.5. Inverse SCOPE model for optical domain

Based on the previous step, the RMSE was used to minimize errors between AHS measured data and simulated spectra from LUT over optical domain in equation 11. The best fit between them was selected to define the best PROSPECT-SAIL parameter for all cases.

$$RMSE = \sqrt{\frac{1}{n}\sum_{i=1}^{n}(R\ measured - R\ simulated)^2} \quad \text{.....11}$$

Where R measured is a measured reflectance at wavelength and R simulated is a model reflectance at the same wavelength, and n is the number of optical bands.

For camelina:

Table 4-2 the input parameters used for building LUTs into SCOPE model.

parameter	Symbol	Quantity	Unit	Minimum value	Steps	Maximum value
Weather conditions				Constant values		
	Z	Height of measurements	m	5		
	Rin	TOC incoming shortwave radiation	Wm^{-2}	745.8		
	Rli	TOC incoming long wave radiation	Wm^{-2}	354.3		
	P	Air pressure	hPa	934.9		
	Ta	Air temperature	C	25.6		
	ea	Actual vapour pressure	hPa	13.1		
	U	Wind speed	ms^{-1}	2.3		
	CO_2	Carbon dioxide concentration	ppm	380		
	O_2	Oxygen concentration	ppm	210		
PROSPECT Leaf parameters	N	Leaf structure parameter	-	0.5	0.1	4
	C_{ab}	Chlorophyll(a+b)content	$\mu g\ cm^{-2}$	0	0.5	2
	C_w	Water content	cm	0.00008	0.00002	0.002
	C_m	Dry matter content	$g\ cm^{-2}$	0.0001	0.0002	0.001
	Cs	Senescent material		0.07	0.01	0.6
SAIL Canopy structure	LAI	Leaf area index	$m^2\ m^{-2}$	0.6	0.1	3
	$LIDF_{a+b}$	Leaf inclination distribution function	-	Fix value(-0.35, -.15)spherical		
	θ_s	Solar zenith angle	deg	Fix value (AHS)= 40.9		
	θ_v	Viewing zenith angle	deg	Fix value(AHS)= 8.08192		
	φ_{sv}	Relative azimuth angle	deg	Fix value(AHS)= 89.2		

For grass:

Table 4-3 the input parameters used for building LUTs into SCOPE model.

parameter	Symbol	Quantity	Unit	Minimum value	Steps	Maximum value
Weather conditions				Constant values		
	Z	Height of measurements	m	2		
	Rin	TOC incoming shortwave radiation	Wm^{-2}	745		
	Rli	TOC incoming long wave radiation	Wm^{-2}	373.2		
	P	Air pressure	hPa	934.9		
	Ta	Air temperature	C	23.9		
	Ea	Vapour pressure	hPa	14.5		
	U	Wind speed	ms^{-1}	2.6		
	Co_2	Carbon dioxide concentration	ppm	380		
	O_2	Oxygen concentration	ppm	210		
PROSPECT Leaf parameters	N	Leaf structure parameter	-	1.2	0.2	2
	C_{ab}	Chlorophyll(a+b)content	$\mu g\ m^{-2}$	10	2	60
	C_w	Water content	cm	0.01	0.01	0.05
	C_m	Dry matter content	$g\ cm^{-2}$	0.0001	0.0002	0.001
	Cs	Senescent material		0.01	0.01	0.1
SAIL Canopy structure	LAI	Leaf area index	$m^2\ m^{-2}$	2	0.5	4
	$LIDF_{a+b}$	Leaf inclination distribution function	-	Fix value(-0.35, -0.15)		
	θ_s	Solar zenith angle	deg	Fix value (AHS)= 40.9		
	θ_v	Viewing zenith angle	deg	Fix value(AHS)= 23.8		
	φ_{sv}	Relative azimuth angle	deg	Fix value(AHS)= 89.2		

For corn:

Table 4-4 the input parameters used for building LUTs into SCOPE model.

parameter	Symbol	Quantity	Unit	Minimum value	Steps	Maximum value
Weather conditions				Constant values		
	Z	Height of measurements	m	5		
	Rin	TOC incoming shortwave radiation	Wm^{-2}	745		
	Rli	TOC incoming long wave radiation	Wm^{-2}	345.3		
	P	Air pressure	hPa	934.9		
	Ta	Air temperature	C	23.9		
	Ea	Vapour pressure	hPa	14.5		
	U	Wind speed	ms^{-1}	2.6		
	Co_2	Carbon dioxide concentration	ppm	380		
	O_2	Oxygen concentration	ppm	210		
PROSPECT Leaf parameters	N	Leaf structure parameter	-	1	0.3	2
	C_{ab}	Chlorophyll(a+b)content	$\mu g\ m^{-2}$	10	5	70
	C_w	Water content	cm	0.01	0.01	0.05
	C_m	Dry matter content	$g\ cm^{-2}$	0.0001	0.0002	0.001
	Cs	Senescent material		0.01	0.014	0.1
SAIL Canopy structure	LAI	Leaf area index	$m^2\ m^{-2}$	2	0.5	3.5
	$LIDF_{a+b}$	Leaf inclination distribution function	-	Fix value(-0.35, -0.15)		
	θ_s	Solar zenith angle	deg	Fix value (AHS)= 40.9		
	θ_v	Viewing zenith angle	deg	Fix value(AHS)= 1.1094		
	φ_{sv}	Relative azimuth angle	deg	Fix value(AHS)= 89.2		

Step 3: Inversion SCOPE model for thermal domain

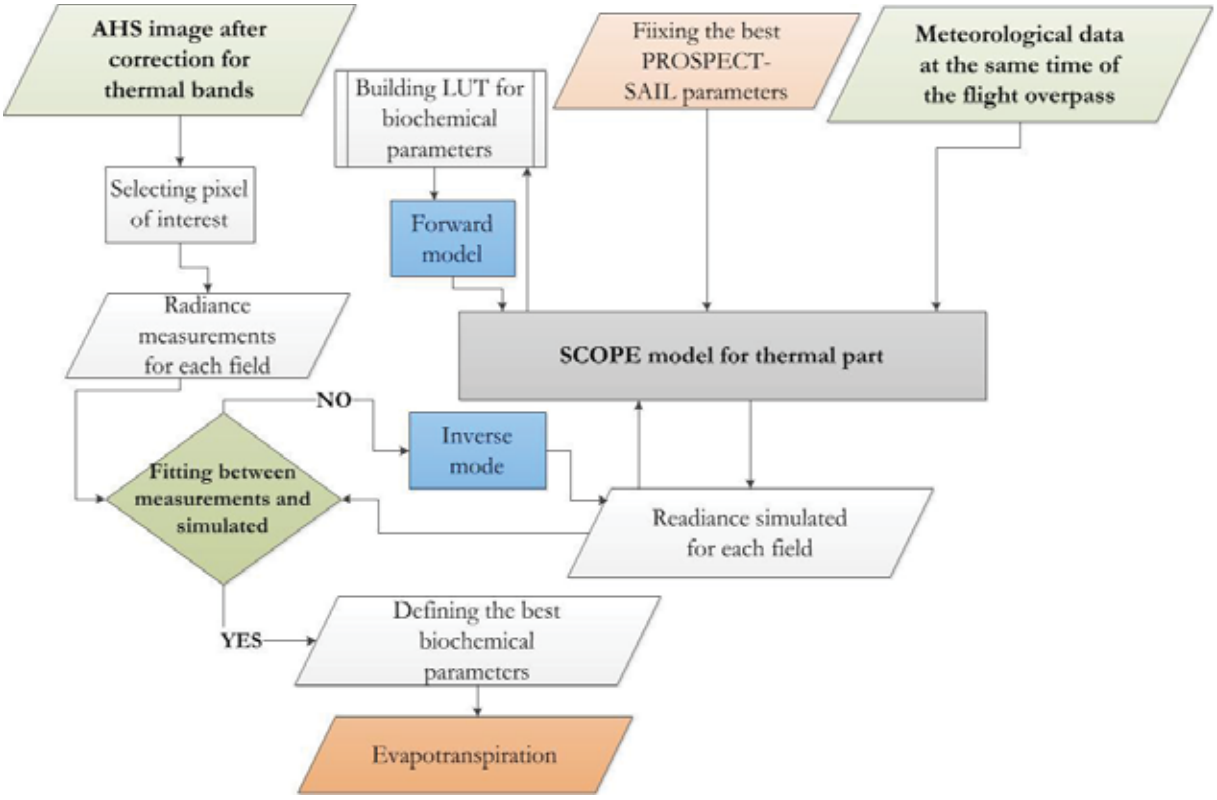

Figure 4-8 Schema the second part of methodology for thermal part

4.6. Forward SCOPE model for thermal domain

From the previous step, the best PROSPECT-SAIL parameters were defined and they will fix facilitation of retrieval biochemical parameters from the thermal domain. The SCOPE model enables using thermal part where the model covers the thermal spectra from (3 to 50 μm). Leaf biochemical parameters and stomatal resistance are used to determine CO_2 and energy fluxes which are affect thermal radiation.

The Vmax as one of biochemical parameters is considered a key parameter in the Farquhar photosynthesis model and it controls carbon fixation process (Farquhar et al., 1980). It varies with type of plant (Wullschleger, 1993), depth in the canopy (Kull et al., 1999), with day of the year (Mäkelä et al., 2004), and weather conditions.
The second variable is m which is slope of the Ball_Berry equation. The m parameter is coupled stomata conductance and relative humidity for C3 plants and C4 plants (Collatz et al., 1991; Steeneveld et al., 2002), see equation 12.

$$gs = m * (\frac{A * rh}{Cs}) + g_0 \quad \text{.....12}$$

Where gs (μmol CO_2 m^{-2} s^{-1}) is stomata conductance, A (μmol CO_2 m^{-2} s^{-1}) is a net assimilation, rh is leaf surface relative humidity, Cs (μmol CO_2 mol^{-1} air) is leaf surface CO_2 concentration and g_0 (μmol CO_2 m^{-2} s^{-1}) is a minimum conductance.
The m parameter plays a vital role for prediction CO_2 and water vapour fluxes. With the different species of plant (C3 & C4), the assimilation of atmospheric CO_2 is affected based on the capacities for the biochemical reactions that regulate the gas changes process (Baldocchi et al., 1998). The stomatal

conductance controls coupling uptake of carbon dioxide and loss of water at the same time which is responding to a set of factors ranging from light intensity to CO_2 concentration as well as leaf water statues (Chaves et al., 2003). (CHAVES, 1991) found that water deficit has a limited leaf fixation of CO_2. The last parameters rbs and rss have a function on soil moisture availability. rss calculates water vapour from soil pores and rbs calculates amount of heat transport and water vapour from soil surface. These parameters contribute the process of exchange of energy and water vapour between the atmosphere and the canopy surface. They are calculated by using an aerodynamic resistance to momentum with the resistance diffused within canopy (rwc) (Wolf et al., 2006).

4.6.1. Sensitivity analysis for thermal domain

In order to determine which parameters are sensitive on the thermal domain, sensitivity analysis achieved this. The dominate ones was selected Vmax, m and rbs. But the other parameters such as rss and rwc don't affect the thermal band as shown in Figure 5-11 to 5-13.

4.6.2. Generation LUTs for thermal domain

Building LUTs were performed based on the sensitivity analysis for biochemical parameters. For each plant, these parameters were defined as range with a regular step with fixation of optical parameters. The physiological status and type of plant should be taken into account, as well as soil condition under specific weather conditions.

Table 4-5: The input parameters of Look up table for retrieval biochemical parameters on the thermal part

Parameters	Camelina			Grass			Corn		
	Min	Steps	Max	Min	Steps	Max	Min	Steps	Max
Vmax (μmol CO_2 m^{-2} s^{-1})	1	1	20	20	10	100	10	10	100
m	1	1	10	10	1	20	10	5	100
rbs (s m^{-1})	25	5	300	10	50	200	5	5	200
Type of plant	C3			C3			C4		
hc (m)	0.5			0.1			2		

4.7. Inverse SCOPE model for thermal domain

The RMSE was used for thermal band to define the minimum error between simulation and measurement of the model and airborne data. The best parameters (Vmax, m and rbs) were determined after getting the best match between them.

$$RMSE = \sqrt{\frac{1}{n}\sum_{i=1}^{n}(R\ measured - R\ simulated)^2} \quad \text{.....13}$$

Where R measured is a measured radiance at wavelength and R simulated is a simulated radiance at the same wavelength, and n is the number of thermal bands.

Step 4: forward SCOPE time series model for retrieval ET daily and validation results with ground data

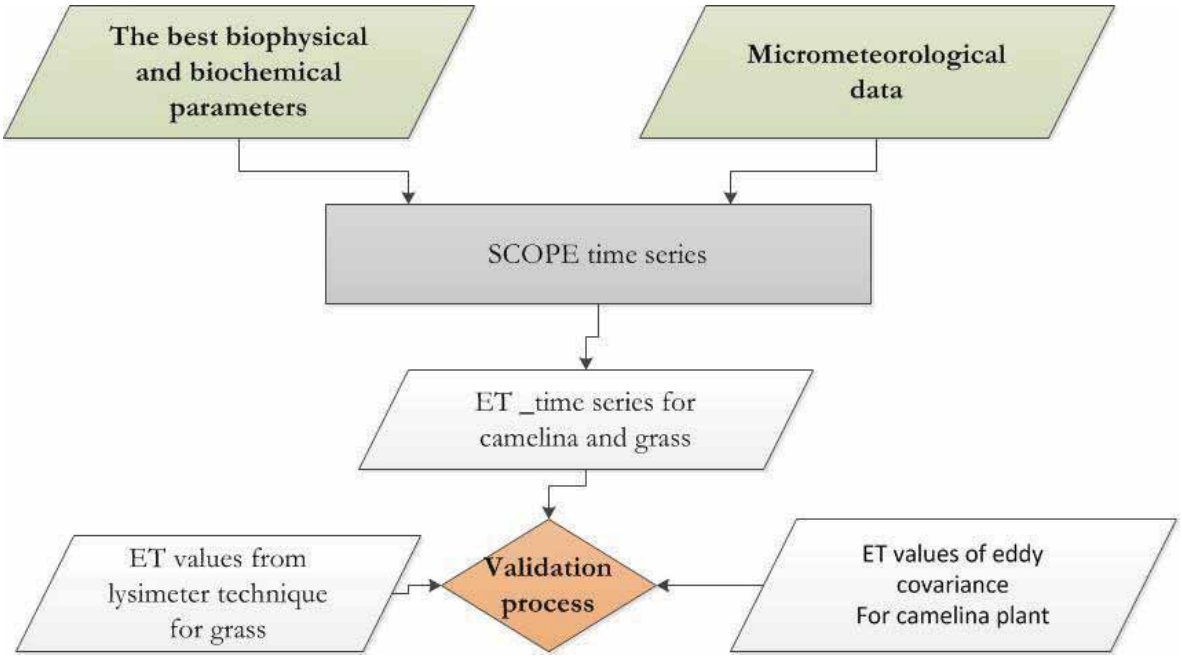

Figure 4-9: The validation process of the SCOPE time series model

4.8. SCOPE model evaluation

The best biochemical and biophysical parameters were obtained from the step 3. It was used into the SCOPE model with the meteorological data as input data. ET daily was generated based on using the SCOPE time series. The results had been tested with the ground data for various field experiments which have different functions in both groups C3 and C4.

For camelina plant, ET daily generated from the SCOPE model was validated with ET daily from eddy covariance (EC) technique. Also, lysimeter technique (Campbell Lisimetro Festucawas) was used for validating results from grass. It is worth to mention that units of ET values generated from model depend on the unit of metrological data. In first case camelina, all input data from micrometeorological data calculated half hourly, so that the output of the model for ET is in mm per 30 minutes. However, second case grass, micrometeorological data calculated hourly so ET values are in mm per hour.

Another potential of the SCOPE model is that it has capability of generation ET from instantaneous data to daily (10 days of EC measurement for camelina and 7 days of lysimeter technique for grass) based on micrometeorological data. Statistical analysis such as RMSE, R^2 was used to define the between the correlation and variation between them.

5. RESULTS

5.1. Pre-processing of AHS data

A complete atmospheric and geometric processing chain is necessary to provide spectral information AHS data; this type of processing is required for many applications especially for vegetation cover under this study to avoid errors.

5.1.1. Atmospheric correction by MODTRAN 5.2.1

Atmospheric correction of air borne hyperspectral data typically consists of two steps for optical and thermal parts. The first step: it is required to retrieve atmospheric parameters especially aerosol optical thickness (AOT) for retrieval the reflectance from the radiance. The second one: thermal radiation was corrected based on the radiative transfer equation for a given AOT. The input parameters of MODTRAN are defined by specifying the AHS flight time, flight altitude, RAA, VZA and SZ angle. The accurate value for visibility will be 30 km (0.2576 AOT) after applying LUTs. In Figure 5-2 and 5-3, reflectance and radiance from the target has been computed after applying AC.

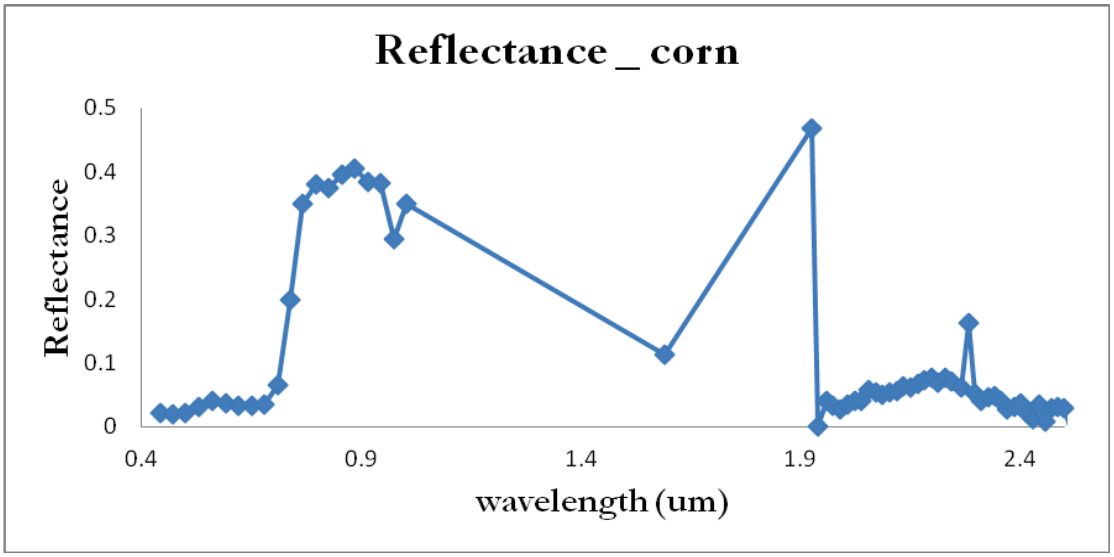

Figure 5-1: The reflectance spectra of AHS data before applying atmospheric correction for corn

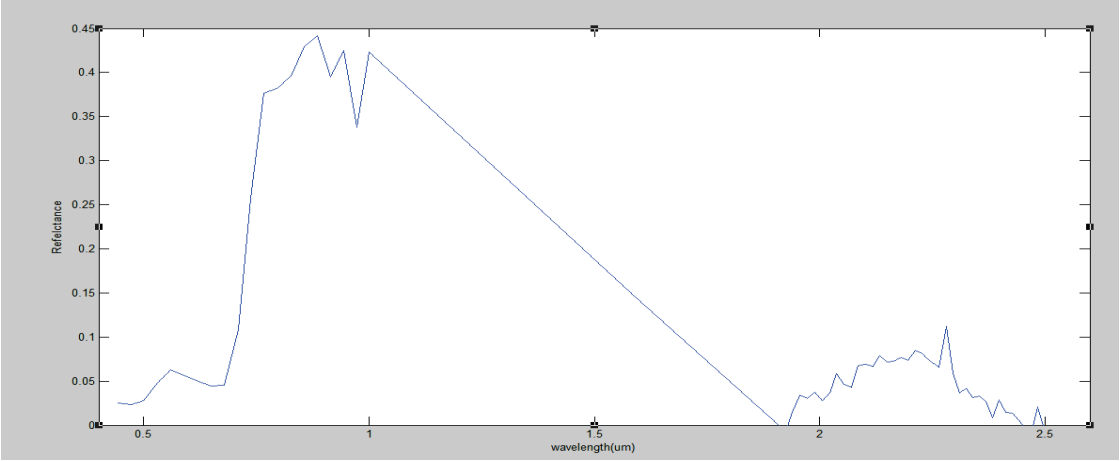

Figure 5-2: The reflectance spectra for corn after atmospheric correction by using MODTRAN 5.2.1

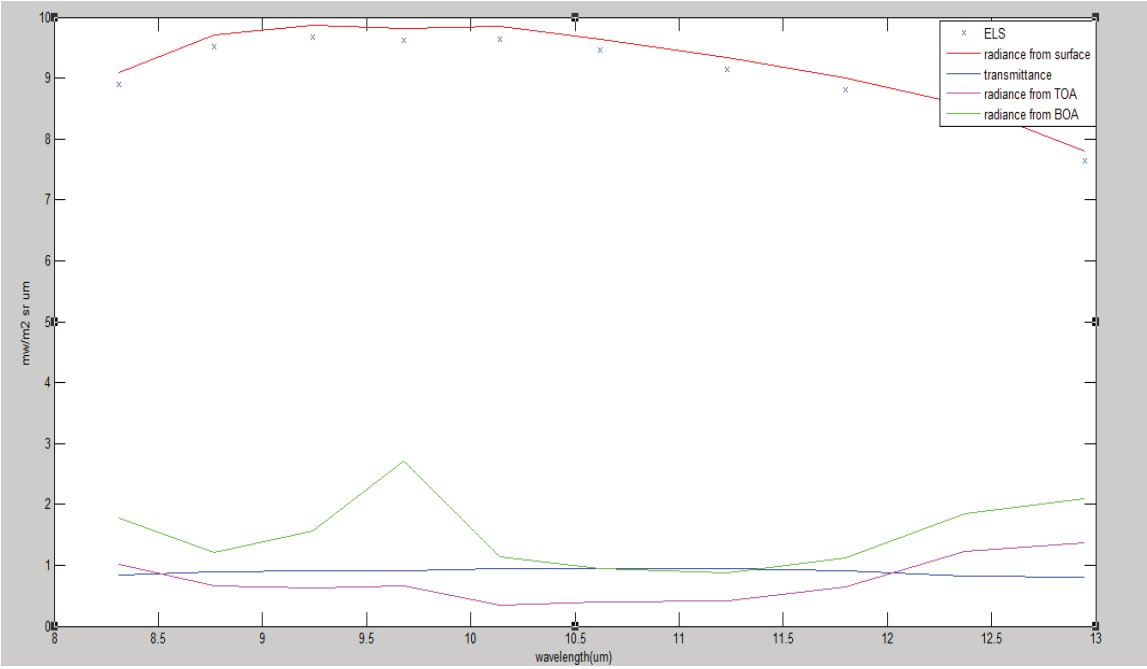

Figure 5-3: The surface radiation from corn after applying atmospheric correction as shown in red line, the blue point is emissivity multiplied radiance, the blue line is transmittance, the green light is radiance from (BOA) and pink line is radiance from TOA.

5.1.2. Geometric correcting

Figure 5-4 shows images before and after geometric correction in order to remove these instabilities by using IGM files. Each pixel after correction has coordinate x and y to identify the location and to be used as input parameter into SCOPE model.

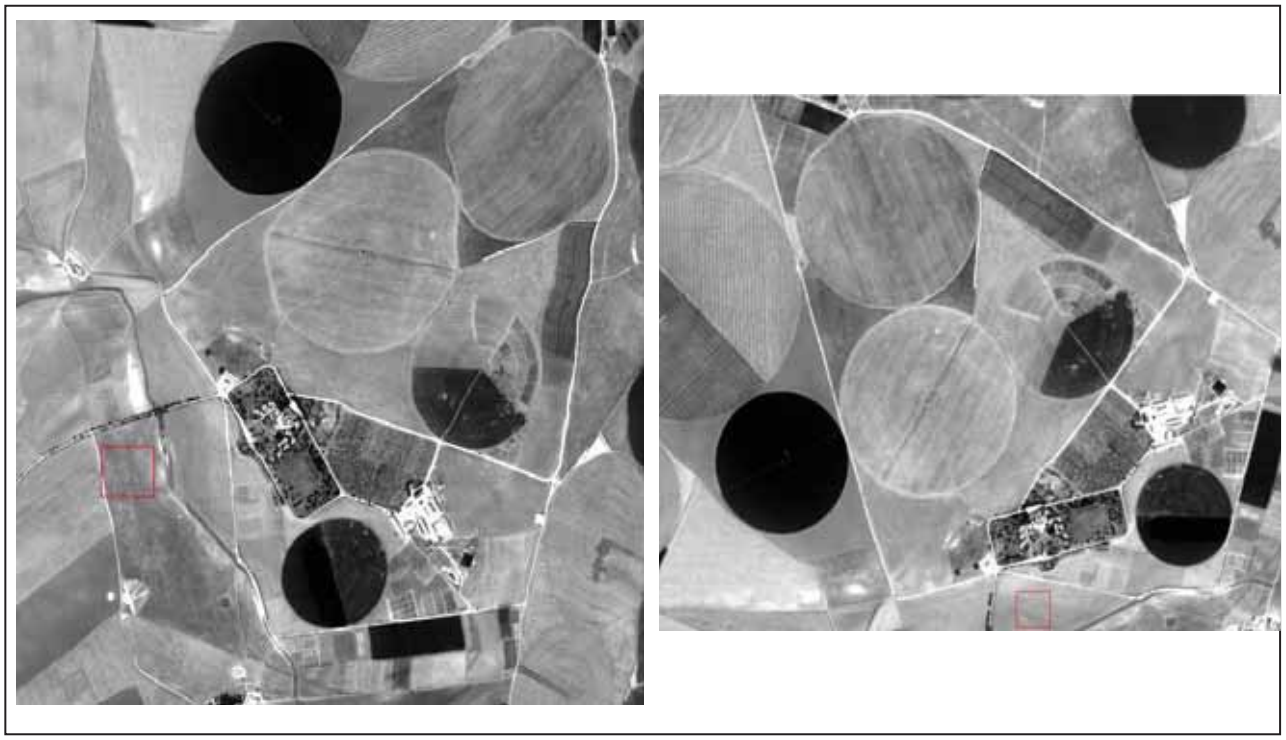

Figure 5-4: Raw AHS data before doing geometric correction (on the left) and AHS data after correction (on the right)

5.2. Sensitivity analysis for biophysical and biochemical parameters

Through this section, the suitable range for each field and the effect of biochemical and biophysical properties of leaf-canopy over the whole spectrum 0.4 to 50 μm can be predicted. The first subsection contains parameters influencing the reflectance and which of them has effect on the spectrum. The second subsection shows the effect of each parameter on the thermal bands. Other parameters were fixed because of insensitivity on the radiation. Figures 5-5 to 5-13 show the quick look of sensitivity analysis.

5.2.1. PROSPECT-SAIL parameters

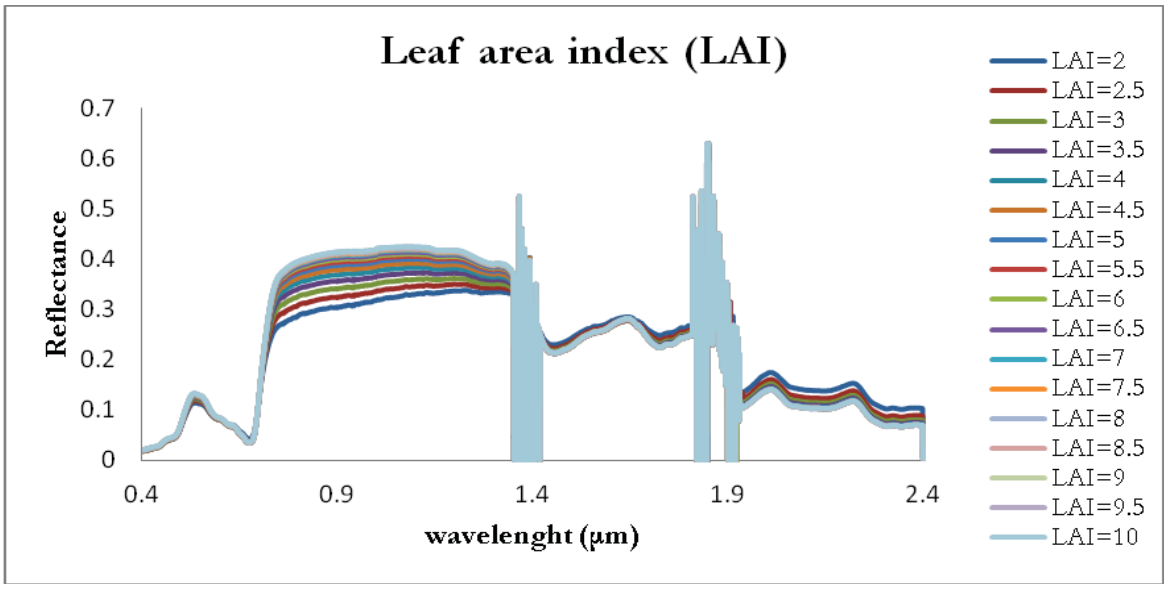

Figure 5-5: The effect of LAI on the Red and NIR band

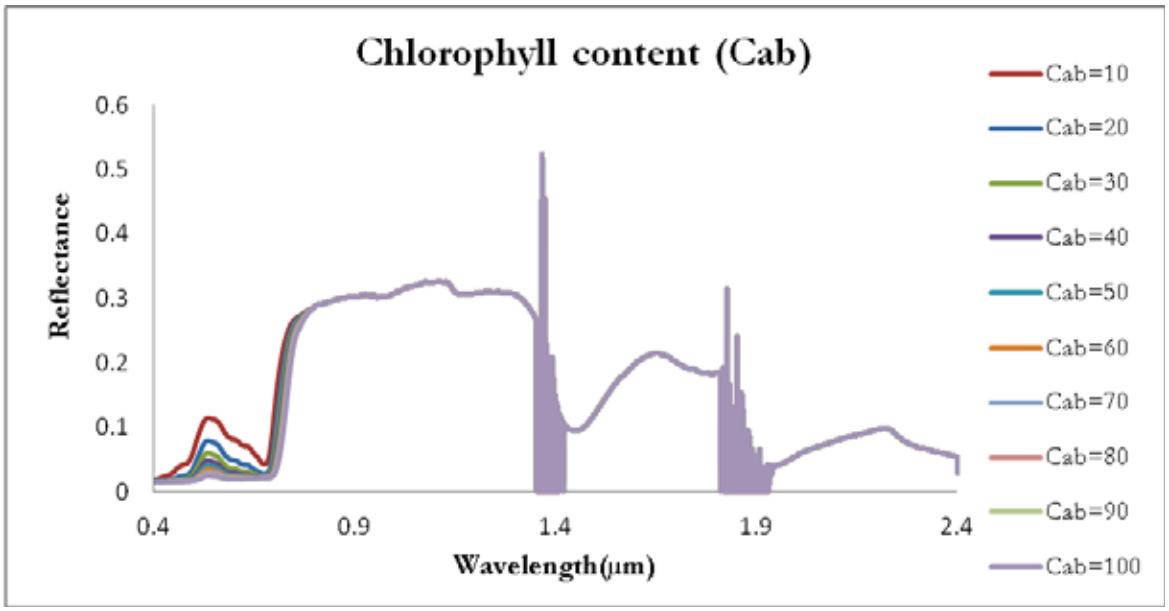

Figure 5-6: The effect of Cab on the VIS band

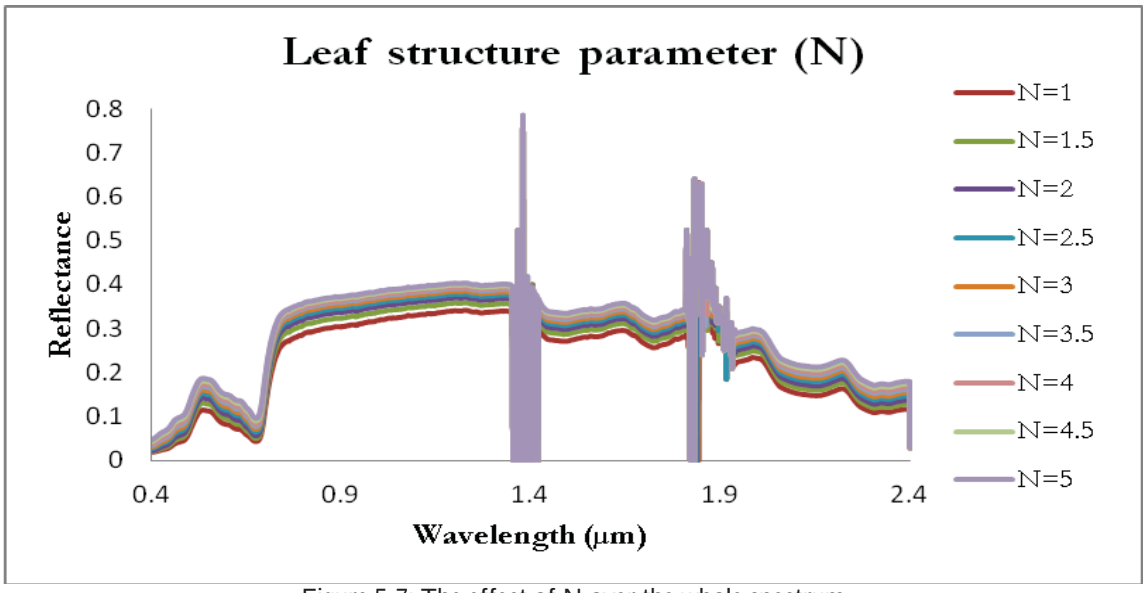

Figure 5-7: The effect of N over the whole spectrum

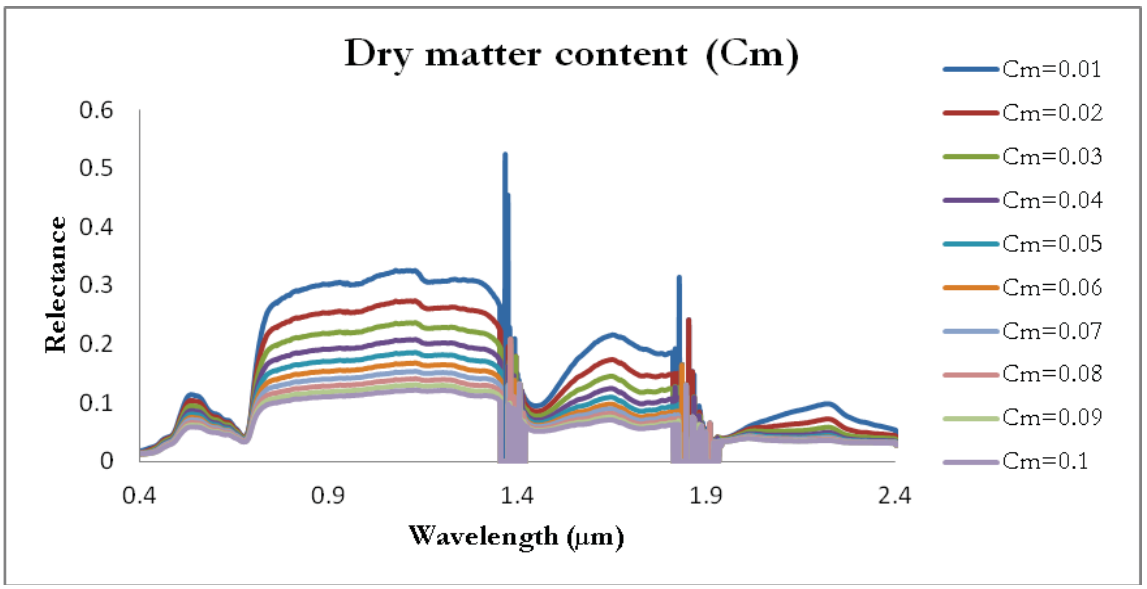

Figure 5-8: The effect of Cm over the whole spectrum

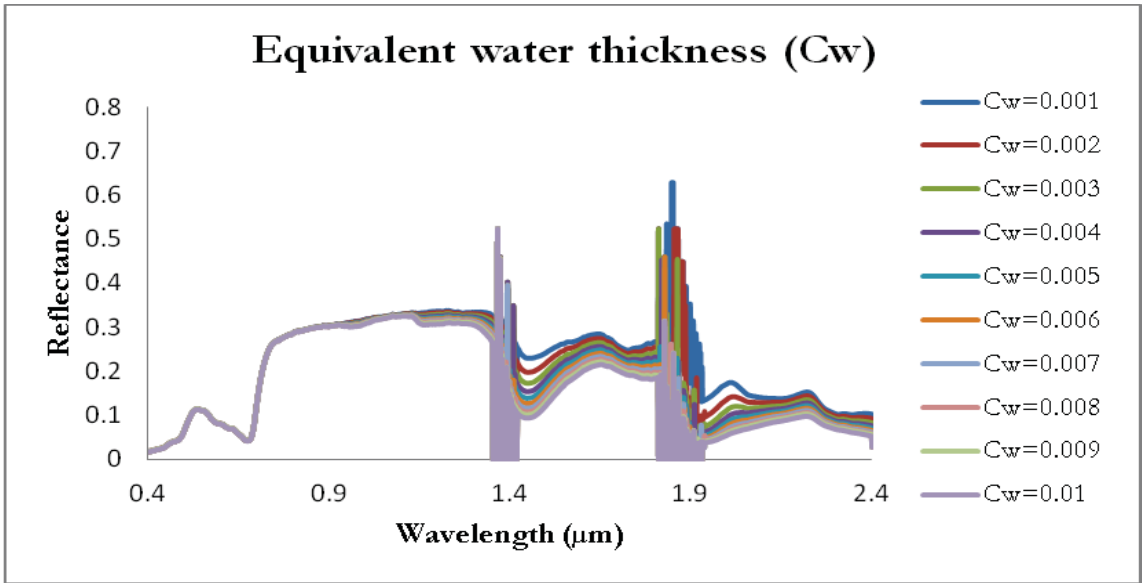

Figure 5-9: The effect of Cw on the SWIR band

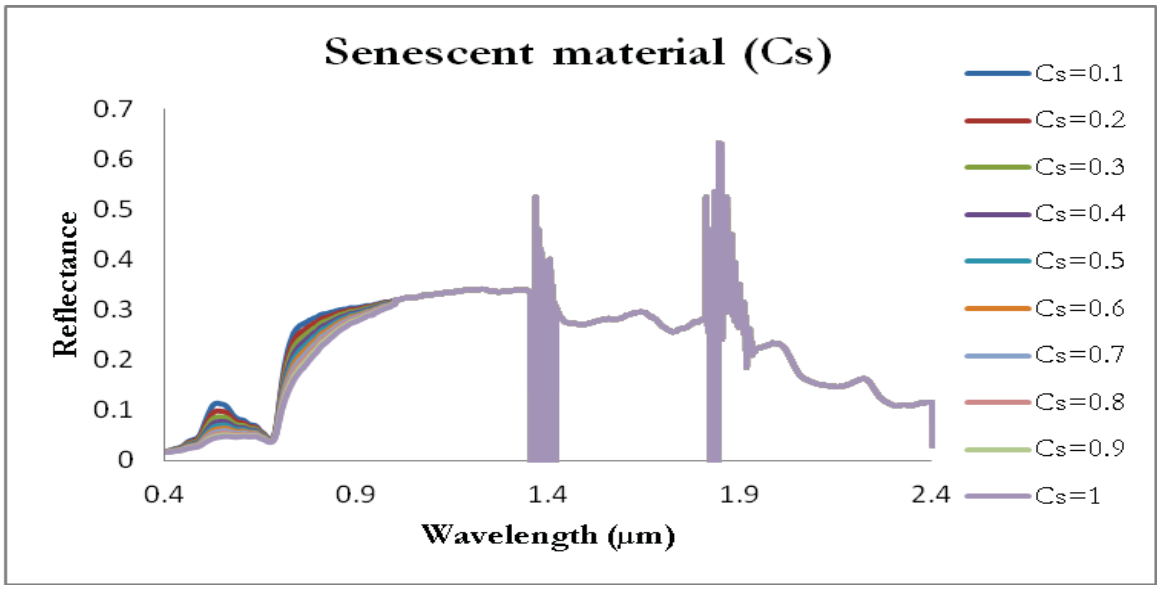

Figure 5-10: The effect of Cs on the VIS + NIR band

5.2.2. Biochemical parameters

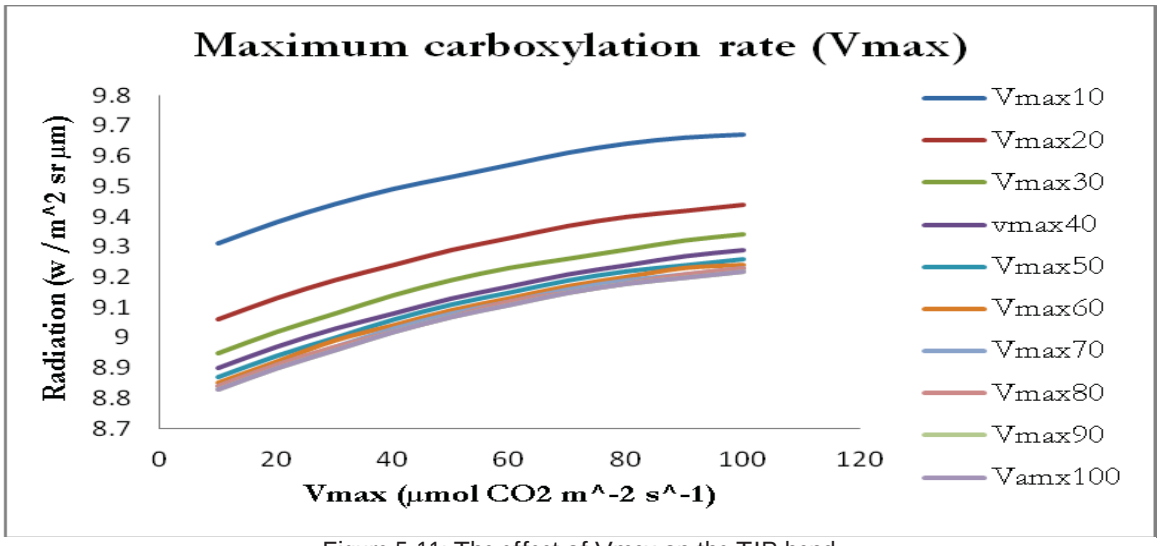

Figure 5-11: The effect of Vmax on the TIR band

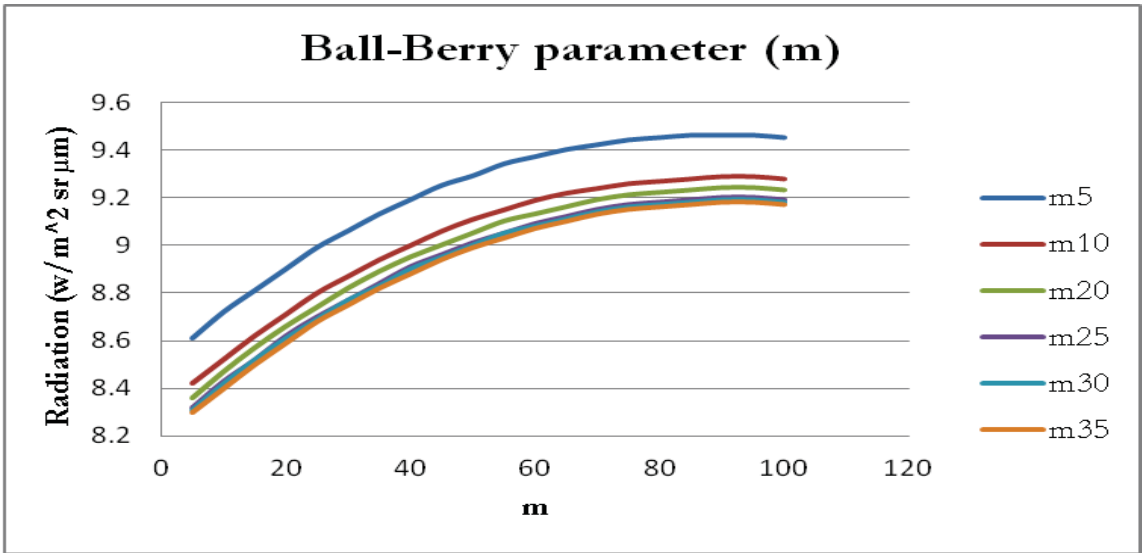

Figure 5-12: The effect of m on the TIR band

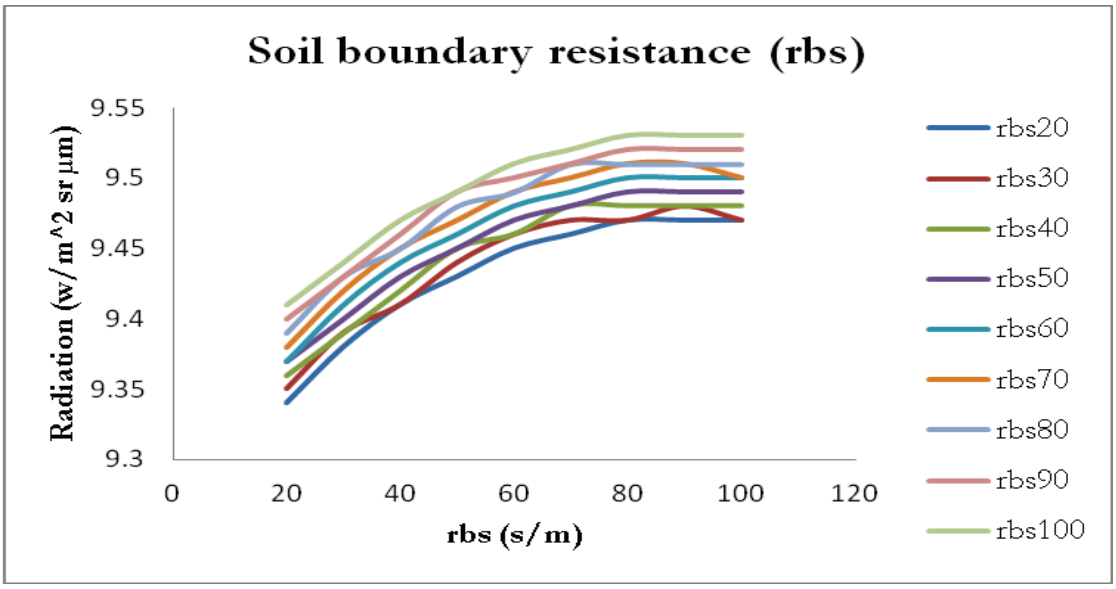

Figure 5-13: The effect of rbs on the radiation

5.3. Estimation PROSPECT-SAIL parameters in optical domain

Steps of retrieving PROSPECT-SAIL parameters are ordered through the following subsections in the same order of the conducted work

5.3.1. Comparison between AHS data and SCOPE model

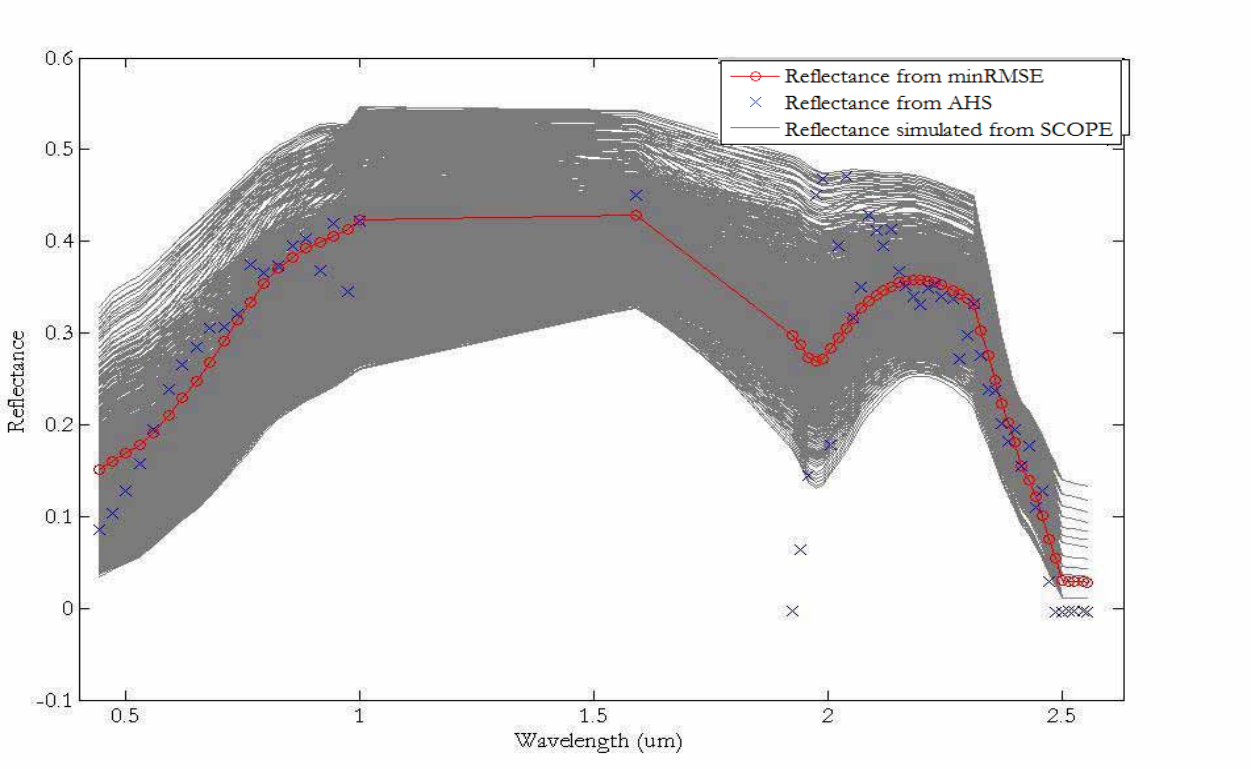

Figure 5-14: Comparison between simulated and measured spectra to define the best reflectance by using RMSE. The red line shows the best fit between them for camelina.

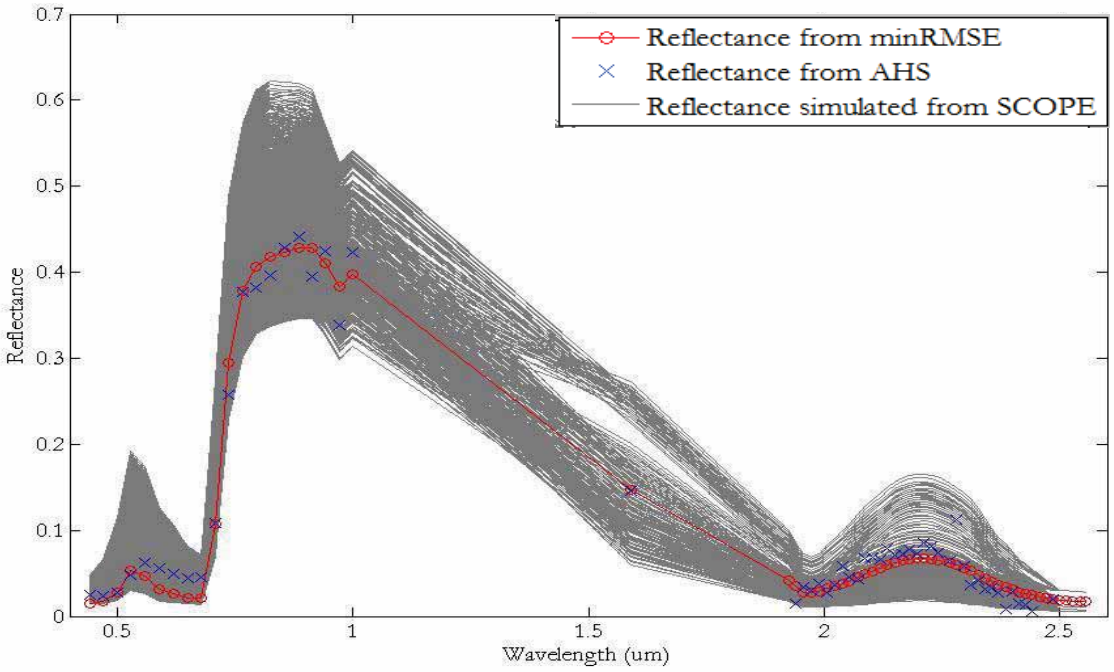

Figure 5-15: Comparison between simulated and measured spectra to define the best reflectance by using RMSE. The red line shows the best fit between them for grass

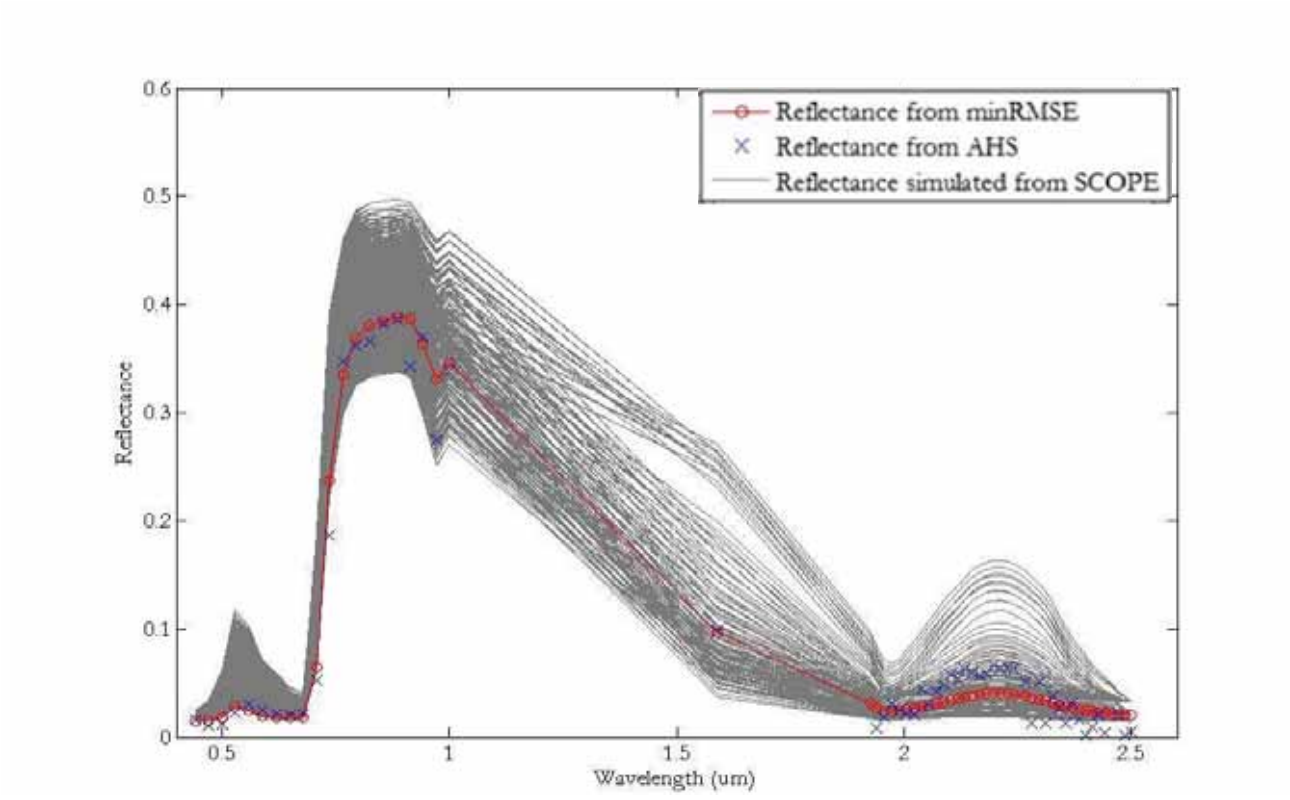

Figure 5-16: Comparison between simulated and measured spectra to define the best reflectance by using RMSE. The red line shows the best fit between them for corn

Figures 5-14, 15 and 16, it is clearly demonstrated that a set of parameter combination lead to match synthetic reflectance with measured reflectance. By using LUT approach, the parameter values are quantified by Matlab as steps within the range. For camelina plant, the simulated reflectance does not matched with measured reflectance in visible band where it is related to photosynthesis pigments

absorbed in this region based on sensitivity analysis applied. It indicates the reflectance of vegetation with a low Cab value not well simulated. For grass, the misfit between measured and simulated spectra in the red region (0.690-0.730 μm) refers to the uncertainty of Cab parameter. Corn has misfit in the SWIR (2-2.5μm) region which is related to water content parameter.

5.3.2. The relation between RMSE with PROSPECT-SAIL parameters

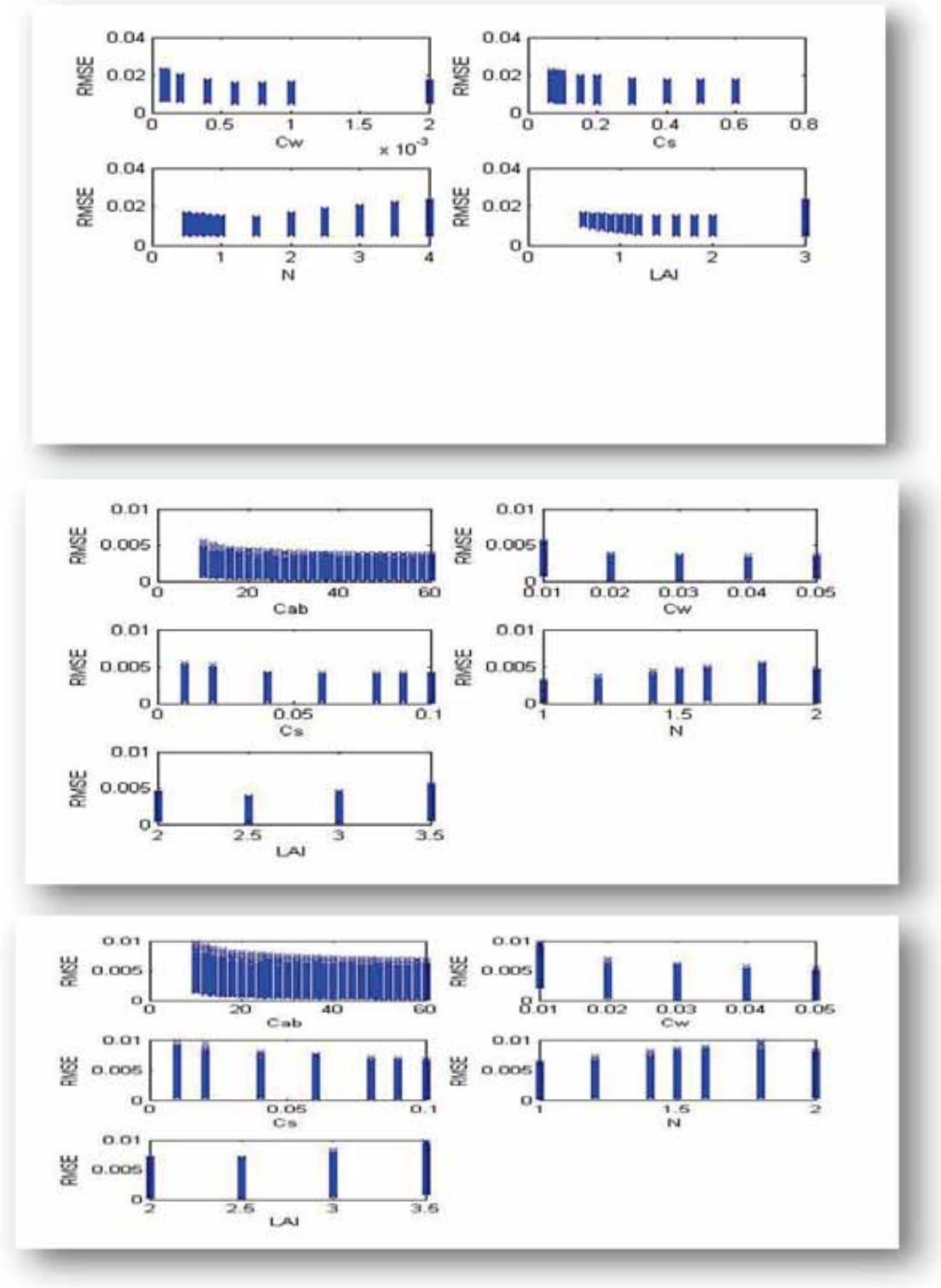

Figure 5-17: The relation between changing RMSE with changing values for PROSPECT-SAIL parameters for camelina, grass and corn respectively.

Figure 5-17 shows that substantial change in RMSE with changing values of each parameter contributes to know the best PROSPECT-SAIL parameters for each plant. Based on this, it is possible to obtain the optimal value during model calibration which has low RMSE.
Corn and grass have high chlorophyll content. However, camelina was in senescence stage having low water content, low chlorophyll content resulting in yellow colour as well as leaf area index has low value. This reflects the inter-correlation between LAI and Cab (Darvishzadeh et al., 2008(b)).

5.3.3. Defining the best PROSPECT_SAIL parameters in optical domain

Table 5-1 shows the optimal estimated parameters for each field, by calibrating synthetic reflectance provided from set of input parameters with measured data.

- Derived Cw parameter for camelina is the lowest value compared to other crops. This agrees with the observation that during the flight overpasses, the plants were dry.
- Cab parameter is very high in corn and grassland and low in camelina.
- LAI parameter is also high in the green crops (grass and maize) and low in the dry vegetation (camelina).
- N and Cs parameter is low in corn and grass and high in camelina.

Table 5-1: The best PROSPECT-SAIL parameters for three types of plant in optical domain

Parameters	Camelina	Grass	Corn
Cab ($\mu g\ cm^{-2}$)	0	50	60
Cw (cm)	0.001	0.03	0.04
Cm ($g\ cm^{-2}$)	0.0006	0.0006	0.0006
N	2.5	2	1
LAI ($m^2\ m^{-2}$)	2	2.5	2.5
Cs	0.3	0.1	0.1

5.4. Estimation biochemical parameters in thermal domain

Steps of retrieving biochemical parameters are ordered through the following subsections in the same order of the conducted work.

5.4.1. Comparison between the radiation simulated from LUTs of SCOPE model with AHS data

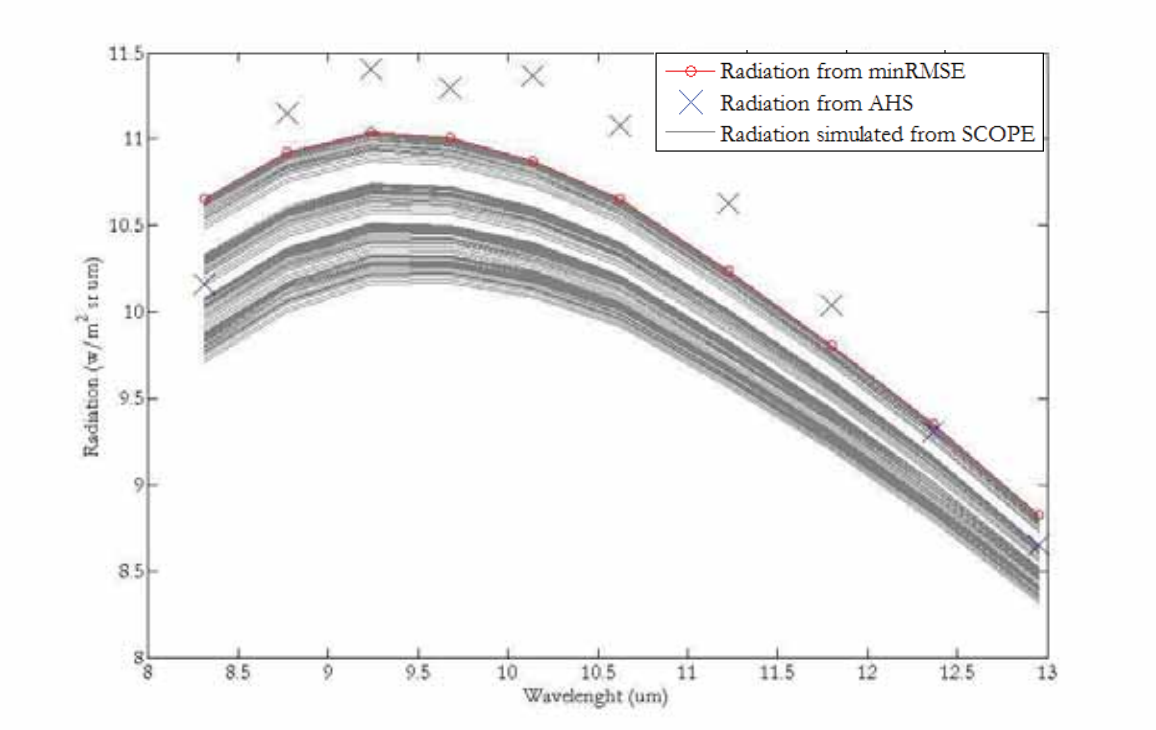

Figure 5-18: Comparison between simulated and measured spectra radiation to define the best radiation by using RMSE. The red line shows the best fit between them for camelina

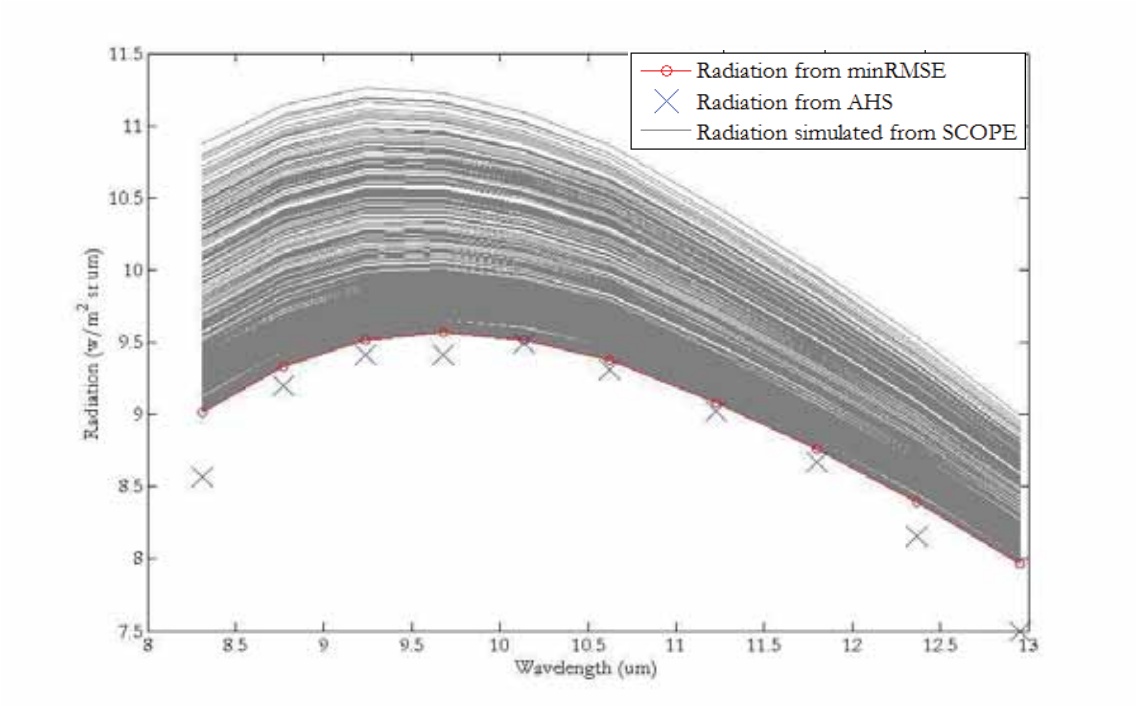

Figure 5-19: Comparison between simulated and measured spectra radiation to define the best radiation by using RMSE. The red line shows the best fit between them for grass

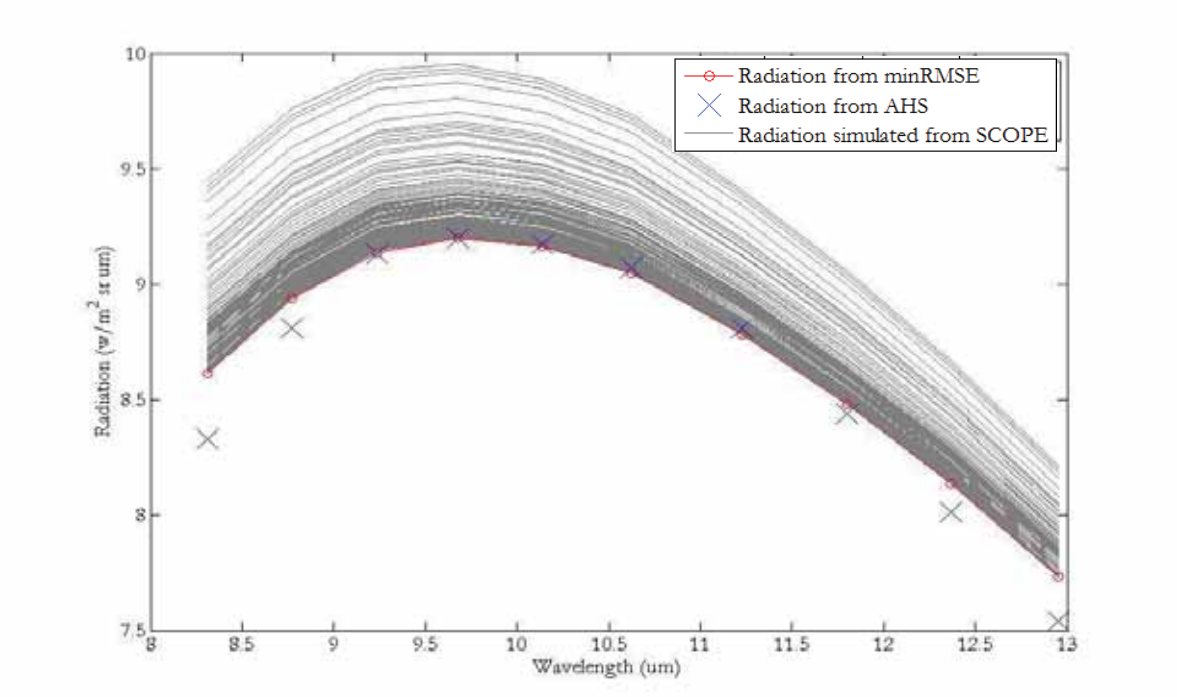

Figure 5-20: Comparison between simulated and measured spectra radiation to define the best radiation by using RMSE. The red line shows the best fit between them for corn

Based on sensitivity analysis conducted on the thermal part, a range of each parameter is assigned for each plant to construct LUTs. LUTs approach were used for simulating radiance and calibrated to match measured AHS data. In the second and last figure for grassland and corn plants (Figures 5-19 and 20), it is clearly seen that radiance simulated from SCOPE model match well with measured data. The synthetic radiance from camelina is not fit with measured data in Figure 5-18.

5.4.2. The relation between RMSE with biochemical parameters

Figures 5-21, 5-22 and 5-23 show the relation between changing RMSE with changing values of each parameter. It can be able to obtain the optimal value which has low RMSE. For camelina, the RMSE reduces with decreasing Vmax and m values. It indicates that the lowest variation between measurement and simulation decreases when value of parameter is close to be correct. Vmax and m are low for dry plants and there are correlations between Cab, Vmax and m parameters. On the contrary, green plants have high values for Vmax and m as shown in Figure 5-22 and 5-23. The RMSE of rbs parameter decreases with increasing rbs value for camelina inversely with green plant where rbs is high for dry soil and low for wet soil.

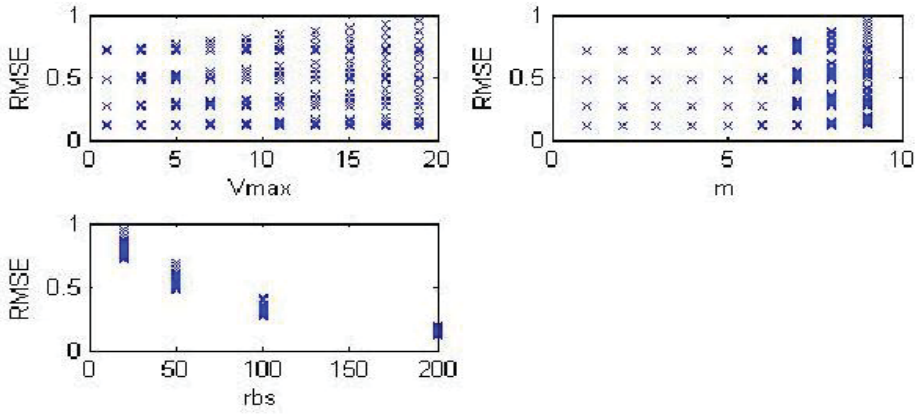

Figure 5-21: The relation between changing RMSE with changing values for each biochemical parameter for camelina

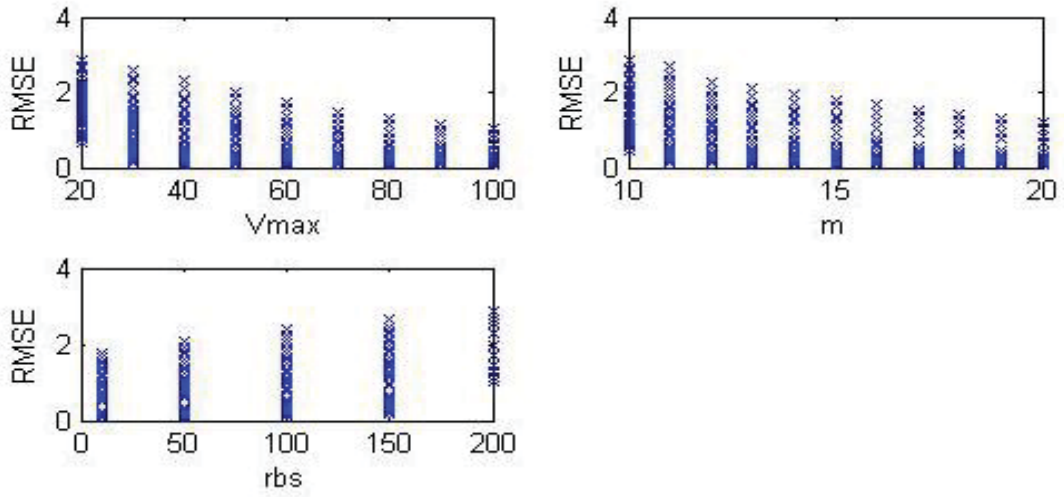

Figure 5-22: The relation between RMSE with changing values for each parameter for grass

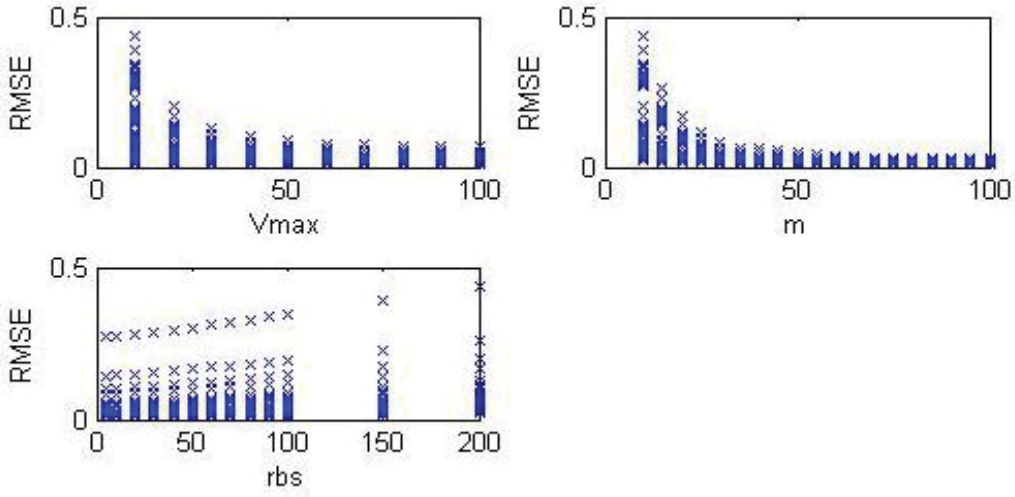

Figure 5-23: The relation between RMSE with changing values for each parameter for corn

5.4.3. Defining the best biochemical parameters for thermal domain

Table 5-2 shows the optimal biochemical parameters in thermal band by fitting the thermal radiation simulated from model with measured AHS data.

- Vmax parameter is very high for vegetation of the C3 photosynthesis pathway than C4 like grass and corn respectively, but low Vmax value in camelina plant.
- Consequently, Ball- Berry parameter (m) is low in camelina plant and high for green plant.
- Soil boundary resistance (rbs) for dry soil is maximum and low for wet soil where it will affect evapotranspiration process.

Table 5-2: The best parameters for three types of plant in thermal domain

Parameters	Camelina	Grass	Corn
Vmax (μmol CO_2 m^{-2} s^{-1})	1	80	60
m	1	18	50
rbs (s m^{-1})	200	10	10

5.5. Validation process for evaluating SOPE model

Based on Defining the best biochemical and biophysical parameters, the SCOPE model can quantify reliable ET by using optical and thermal domain.
Table 5-3 shows the estimation of ET hourly for each plant. Corn has high evapotranspiration compared to grass and camelina.
To validate the performance of SCOPE model, ET simulated from model was compared with the ground data. Table 5-4 and 5-5 shows ET daily generated from SCOPE time series model with ET daily from ground data. For grass, ET daily measured from lysimeter is close to ET daily simulated from SCOPE model. While For camelina, ET daily measured from EC is higher than ET daily simulated from SCOPE model.

Figure 5-24 and 5-25 shows the correlation between ET measured with ET simulated. For grass, there is a good correlation between them. For camelina, there is correlation between them but it is not positive. It refers to instability of weather condition on the last days.

Table 5-6 shows the R^2 and RMSE for camelina and grass. R^2 used to show how much the ET generated from model close to ET measured. RMSE used to show how much the variation between ET simulated and measured. It can be conclude that there is no big variation between ET measured and model for grass but for camelina there is variation on the last day.

Table 5-3 Estimation evapotranspiration during the flight overpass

Time over the flight overpass (DOY)	ET for camelina (mm/h)	ET for grass (mm/h)	ET for corn (mm/h)
207.40	0.00043	0.42878	0.86977

Table 5-4: Comparison between ET daily generated from SCOPE model with lysimeter data for grass

DOY	SCOPE model _ET (mm/d)	Lysimeter _ET (mm/d)
204	7.42	9.02
205	6.38	8.09
206	7.72	7.96
207	8.23	8.47
208	8.21	9.26
209	7.28	8.01
210	5.89	6.49
211	5.44	7.82

Table 5-5: Comparison between ET daily generated from SCOPE model with EC data for camelina

DOY	SCOPE model _ET (mm/d)	Eddy covariance _ET (mm/d)
200	0.023	0.035
201	0.018	0.422
202	0.025	0.767
203	0.022	0.146
204	0.019	0.411
205	0.013	0.583
206	0.021	0.960
207	0.021	0.741
208	0.019	0.583
209	0.013	2.244
210	0.005	2.319

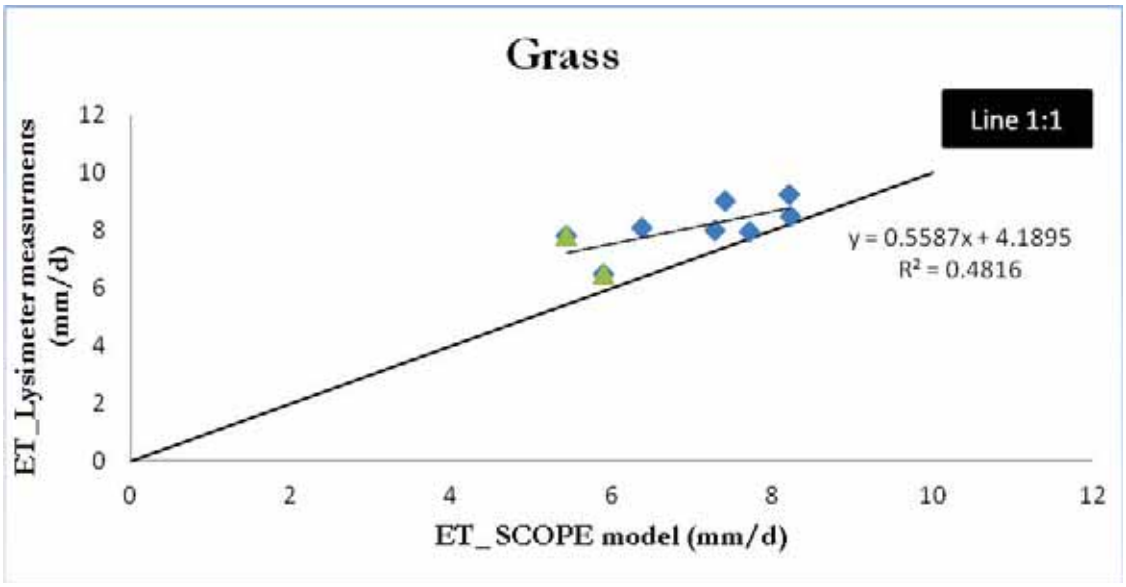

Figure 5-24: Correlation between ET daily simulated from SCOPE model with the ET daily from lysimeter for grass and two points shows ET after a rainfall event in green colour

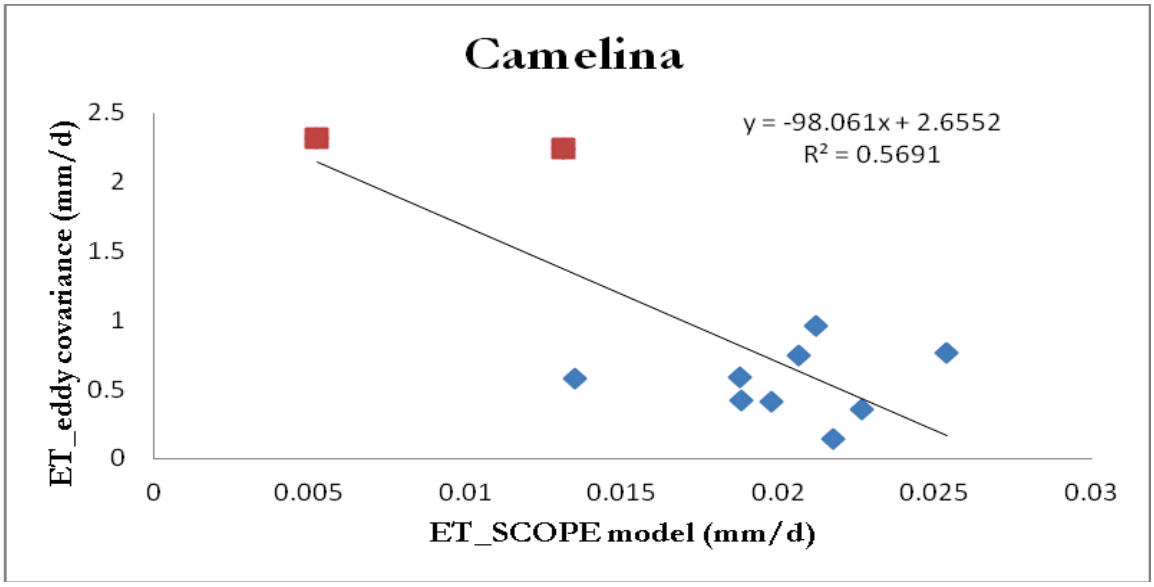

Figure 5-25: Correlation between ET daily simulated from model with the ET daily from eddy covariance for camelina and two points shows ET after a rainfall event in red colour

Table 5-6: The comparison between two types of plants based on statistical analysis

Statistical analysis	Grass	Camelina
R^2	0.49	- 0.54
RMSE (mm/d)	0.24	1.10

Figure 5-26 for grass shows the changing ET with DOY. It can be noticed that The ET trend of SCOPE model is the same pattern of ET measurement. ET of SCOPE model was underestimated. It indicates that on the thermal band, there is uncertainty of estimating land surface temperature.

In Figure 5-27 for camelina, ET simulated from model is so low compared to ET measurement. In addition, the trend of ET model follows the same pattern of ET measurement except the last days. There was rainfall event so that ET from EC starts increasing. ET measurement is high because soil start to evaporate.
rbs parameter (s m^{-1}) starts to decrease gradually which represents transport heat and water vapour to the air.

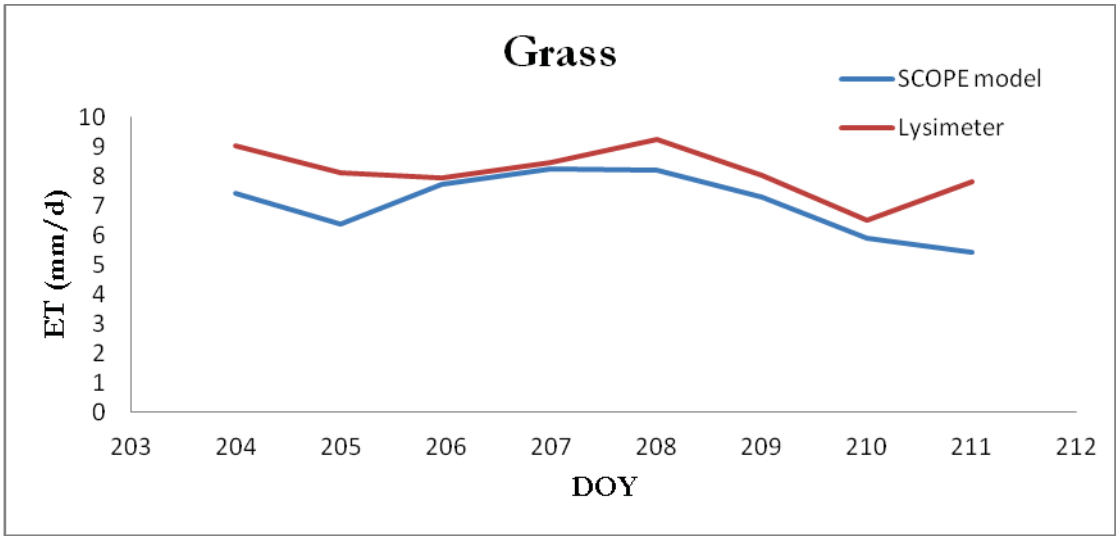

Figure 5-26: The trend of ET daily from SCOPE model and lysimeter measurement with DOY

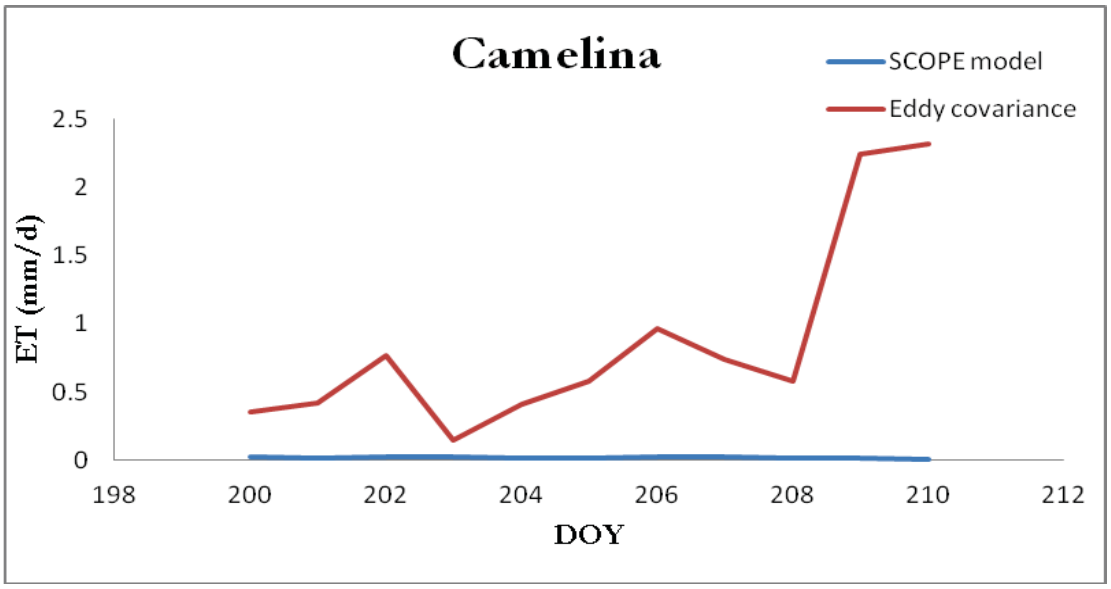

Figure 5-27: The trend of ET daily from the SCOPE model and EC measurement with DOY

6. DISCUSSION

This study was carried out to quantify evapotranspiration from high resolution airborne hyperspectral data with SCOPE model on a pixel bases. This study evaluated the capabilities of SCOPE model for retrieval accurate ET by validating the results with in-situ measurements.

6.1. Data quality

In order to benefit from the potential of SCOPE model as an inverse model, it requires sufficient number of spectral band with high spectral resolution. This spectral information from image should be accurate to get realistic values. It indicates that the performance of model inversion technique depends on the quality of airborne data used. The critical step is the atmospheric correction. It may contribute some errors if images are not corrected well. It is necessary to validate results with ground data correctly. For calculating ET as one of biophysical processes, it was estimated by calibrating spectra information from AHS data and LUTs to define the best biophysical and biochemical parameters. The spectral information was corrected by MODTRAN 5.2.1 based on radiative transfer equation. On the thermal domain, the emissivity for green plant was assumed to be 0.98 and for dry plant 0.91. These values are not realistic values which are the main reason for the uncertainty of ET where each pixel has a different emissivity with different band.

6.2. Sensitivity analysis

During calibration process, sensitivity analysis was implemented to get the knowledge which parameters are sensitive on the spectral information (Haile, 2005). It was done based on varying the values of biophysical and biochemical parameters. SCOPE model has numerous numbers of input parameters for calibration but the major ones were selected.

For optical part, several values of the PROSPECT-SAIL parameters (LAI, Cw, Cm, Cs, N, and Cab) were used to determine the sensitivity on the simulated reflectance. Figure 5-5 shows that the variation of LAI will affect the red and NIR bands. LAI is the ratio of one side of leaf area per ground area and is one of SAIL. It influences the atmosphere and biosphere exchange of CO_2 (Bonan, 1993). The green plant has high LAI therefore it will simulate high reflectance such as grass and corn. The Cab parameter is one of PROSPECT and it is inter-correlated with LAI. As shown in Figure 5-6, the peak of the reflectance in the visible part decrease with increasing Cab value. Cab value will be high when the light absorption increases. (Wu et al., 2008) observed that Cab is a good indicator for vital plant based on photosynthesis process, mutations, stress and nutritional state such as grass and corn. The second parameter of leaf optical properties is Cw. It affects the SWIR and NIR in Figure 5-9. It illustrated that the effect of decreasing amount of water in the leaf will increase the reflectance. Camelina is in senescence stage so that it is suffering from drought. However, grass and corn is fresh plant and has high amount of Cw. Figure 5-8 illustrates the variation of N from low to high on the whole spectrum and it is a good indicator to indentify the vegetation type. It means that N parameter will be high for dry plant and low for green. However, the variation of simulated reflectance isn't big differences. Cm changes with different type of plant. Figure 5-7 is shown that the increasing Cm value will decrease the reflectance on the whole spectrum. Cs is sensitive on the VIS and NIR in Figure 5-10. It shows the variation on the shoulder curve of NIR with changing the peak in the visible. Cs is a good indicator for the stage of growth plant. Camenlina is senescence stage so Cs value will be high with the low reflectance. On the contrary, grass and corn are in maturity stage and have low value of Cs during the flight overpasses.

For thermal part, the biochemical parameters are sensitive on the thermal radiation. The most dominate ones are Vmax, m and rbs after applying sensitive analysis. Parameter rbs indicates amount of heat and water vapour transport from surface soil so that wet soil has low rbs and vice versa. Figure 5-13 shows that thermal radiation increases with increasing rbs (s m^{-1}) value.
The m parameter is a function of stomatal conductance and relative humidity. It indicates that during the normal condition, the stoma will open especially in the morning and start to uptake CO_2 and transpire water but in the afternoon or under drought condition, the stomata will close. Figure 5-12 shows that the thermal radiation decreases with increasing m. The Vmax parameter follows the same trend of m parameter where it will increase with decreasing thermal radiation. As mentioned before, it represents plant photosynthetic capacity and used to predict photosynthesis rate of plant. Vmax is higher for green plant compared to dry plant.

6.3. Estimating the best biophysical and biochemical from inverse SCOPE model

A simulation study was conducted to study the spectral capability of AHS for retrieval parameters based on inverse SCOPE model. The mismatch between simulation and measurement of the model and airborne data is considered as a source of errors. These errors are associated to biophysical model and inversion approach used. The SCOPE model is a complex model and it was formed through a combination of three modules. It has many parameters which needed to be parameterized. The implemented LUT method contributes also some errors (Williams, 2012). The size of LUT has also big limitation where there is increasing size of LUT. Simulations will take much time during running the model (Williams, 2012). These simulated spectra are based on combination of input parameters. Some parameters are affecting each other.

For optical part, it was found that when the thermal radiation generated from the model compared to AHS data, there is mismatch in (visible and NIR region) of camelina. Both visible and NIR bands have a relation to LAI and Cab parameters. Accordingly the relation between LAI and Cab parameters is proportionate, so if Cab parameter result is low value, LAI parameter should be low. For corn, SWIR region is different in both the model and AHS data which is related to Cw parameter. In addition, grass has misfit in the red band which is related to Cab and LAI. Generally from all these errors could be caused by view - illumination geometry effects, atmospheric error, calibration errors and background underneath the canopy (Fernandes et al., 2003; Shabanov et al., 2005; Wang et al., 2001; Yang et al., 2006).

For thermal part, the SCOPE model in thermal domain is used to simulate fluxes. Based on sensitivity analysis, it was found Vmax, m and rbs are used for optimization. These parameters have a significant impact on ET simulated. Vmax and m vary with responding to environmental conditions such as air temperature, relative humidity and intensity of light. From these results, there was found the best match between measured and simulated for grass and corn on the thermal bands. However, for camelina there is misfit between measured and simulated on the thermal bands. Consequently, estimation of the best biochemical parameters is not accurate. This error could have been caused by emissivity value or miss-parameterization for other parameters.

The m parameter is a function of stomata conductance which is related linearly to photosynthesis (Zhang, 2010). Stomata conductance controls the inward diffusion of CO_2 and the outward diffusion of water so that it is required to estimate m and Vmax accurately. These parameters start to decline when soil moisture content decrease (Ju et al., 2010). It means that stomata conductance, photosynthesis conductance responses in parallel to daily changes in soil water content and temperature (Xu et al., 2003). After the flight overpass, there was a rainfall event. Soil moisture increases gradually and stomata starts to open for transpiration process. Therefore, Vmax and m parameter start increasing as in the case of grass

and corn. However, in case of camelina it was yellow and senescence stage. It means no stomata to do photosynthesis process. Vmax and m are very low. In the case of grass and corn, the previous studies found that Vmax and m varied from 3 to 24 under normal condition (Wolf et al., 2006). The m parameter is 50 for corn and 18 for grass. Vmax value is 60 (μmol CO_2 m^{-2} s^{-1}) for corn and 80 (μmol CO_2 m^{-2} s^{-1}) for grass. rb value is high for camelina and low for corn and grass. Value of rbs is 10 (s m^{-1}) for grass and corn because of wet soil but is 200 (s m^{-1}) for camelina on dry soil.

6.4. Validating ET model with ground data

From the results, it was found that green plant has high ET compared to dry plant. The model gives acceptable results in case of green plant and for camelina. By regarding R^2 and RMSE, grass shows good correlation with low value for RMSE but for camelina, R^2 has a negative correlation with high value for RMSE. There is a negative correlation because of the rainfall event on the last days and soil moisture start to evaporate.

SCOPE time series was used to simulate ET time series based on constant values of input parameters. For camelina, rbs is high for dry soil before rainfall but after rainfall rbs starts decreasing.

In Figure 5-26, it was found that the trend of ET daily simulated from model follows to the ET daily measured from lysimeter. There is Small variation between them due to emissivity value. There is a good match between thermal radiation from LUTs and measured data.

In Figure 5-27, for camelina, ET simulated from model is close to zero because of evaporation at comes from soil not from plant. In addition, there is variation between the trend of ET measured and simulated because of misfit between the thermal radiation generated from SCOPE model and AHS measurement.

In order to improve the correlation, the emissivity from AHS should be accurate value not from the previous studies. Furthermore, more parameters need to be parameterized such as rss parameter which is responsible for evaporation process from soil. Finally, all these errors will affect ET simulation. Based on this the quantification of these errors, it will be useful for adaption of SCOPE time series model.

7. CONCLUSION AND RECOMMENDATION

7.1. Conclusion

The main objective of this research was to evaluate the capability of SCOPE model for estimation of evapotranspiration for different crops in Barrax, Spain. To achieve this, meteorological data and remote sensing data from airborne hyperspectral scanner were analyzed. Accordingly, evapotranspiration was estimated from the model and this was also validated with the ground truth data. Based on the findings, the following conclusions are pointed out.

Sensitivity analysis was performed for biophysical and biochemical parameters in the optical and thermal parts. Based on the analysis, it was found that 6 parameters (LAI, Cab, Cw, Cdm, Cs and N) are sensitive on the reflectance while 3 parameters (Vmax, m and rbs) are sensitive on the radiation. Each of them has high sensitivity in a specific band. Based on this, the acceptable range for each parameter was estimated and this was also used for generation of LUTs. From the generated LUTs the spectral information for each of the three vegetation types was simulated. Therefore, the spectral information from the LUTs can be used for calibration of AHS data.

In order to retrieve realistic values of reflection and radiation from image, pre-processing of AHS data was done. In this case, atmospheric and geometric correction was applied. During the pre-processing it was found that the data quality of AHS introduced some errors on the thermal bands due to assumed surface emissivity value. However, reliable results were found for reflectance bands. Consequently the AHS data in thermal band gave inaccurate results.

Comparison of spectral information from AHS data with that of LUTs for retrieval of the best biochemical and biophysical parameters was performed and this was conducted using RMSE. For PROSPECT-SAIL parameters, the result of the comparison revealed that there were miss matching values for grass and camelina in the visible band and in the short wave infrared band for corn of the optical parts. However it showed best fit in the other bands of the optical part. The best fitting results were observed for corn and grass on the thermal part. However, the miss match results were observed for camelina.

After defining the best biophysical and biochemical parameters, SCOPE model was able to quantify ET for each plant. From the results, it was found that the corn has high ET compared to the others at the flight overpass.

Finally, the ET values from the SCOPE model were validated by using ground data for grass and camelina. The validation was carried out using R^2 and RMSE and the results show that good correlation with R^2 value of 0.48 and RMSE value of 0.28 (mm d^{-1}) for grass. However, negative correlation with R^2 value of - 0.56 and RMSE value of 1.1 (mm d^{-1}) was found for camelina. This was due to the rainfall event after the flight overpass. Therefore, the SCOPE model can provide accurate results of ET for grass and camelina during normal condition. On the other hand, it cannot provide accurate results of ET during rainy days.

7.2. Recommendataion

The performance of SCOPE model gave acceptable results. However, it still needs some improvement if the following recommendation will be undertaken:

- To improve the results from SCOPE model, it is required to provide AHS data with the high quality carried by the Spanish Institute of Aeronautics (INTA) under REFLEX campaign.
- The lack of providing ground data for atmospheric measurement and for radiometric measurements has effect on results. Ground data is recommended to reproduce accurate values from AHS data.
- To improve the accuracy of ET values for plants, it is required to estimate accurate value of emissivity. It can be estimated by using TES algorithm which is based on separation emissivity from land surface temperature (Sobrino et al., 2006).
- Biophysical and biochemical parameters retrieved from the SCOPE model should be validated with the ground data. In order to achieve this, a field survey can help to provide real values.
- For the SCOPE model, it has disadvantages because of that the highly number of parameters need to parameterize and lead to highly complex model. With taking into account, the model should be simplified for users and represent the real world.
- For improvement the SCOPE model, it is required to validate this model with other models.
- SCOPE model was built for 1D vertical dimension with ignoring the variation in horizontal direction so that the model needs to improve to 3D dimension for heterogeneous area.
- Furthermore, SCOPE time series model should be considered the changing of soil condition during the day.
- For further study, the SCOPE model should be performed for the whole scene not only for one pixel to study the spatial variability.

LIST OF REFERENCES

Aires, L. M., Pio, C. A., & Pereira, J. S. (2008). The effect of drought on energy and water vapour exchange above a mediterranean C3/C4 grassland in Southern Portugal. *Agricultural and Forest Meteorology, 148*(4), 565-579. doi: 10.1016/j.agrformet.2007.11.001

Allen, R., Pereira, L., Raes, D., & Smith, M. (1998). *FAO Irrigation and Draninage Paper*. Rome, italy.

Baldocchi, D., & Harley, P. C. (1995). Scaling carbon dioxide and water vapour exchange from leaf to canopy in a deciduous forest. II. Model testing and application. *Plant, Cell & Environment, 18*(10), 1157-1173. doi: 10.1111/j.1365-3040.1995.tb00626.x

Baldocchi, D., & Meyers, T. (1998). On using eco-physiological, micrometeorological and biogeochemical theory to evaluate carbon dioxide, water vapor and trace gas fluxes over vegetation: a perspective. *Agricultural and Forest Meteorology, 90*(1-2), 1-25. doi: citeulike-article-id:5693526

Baret, F., Weiss, M., Trouflen, D., & Combal, B. (2000). Maximum information exploitation for canopy characherization by remote sensing. *Aspects of Applied Biology, 60*, 71-82.

Bonan, G. B. (1993). Importance of leaf area index and forest type when estimating photosynthesis in boreal forests. *Remote Sensing of Environment, 43*(3), 303-314. doi: http://dx.doi.org/10.1016/0034-4257(93)90072-6

Box, E. (1978). Geographical dimensions of terrestrial net and gross primary productivity. *Radiation and Environmental Biophysics, 15*(4), 305-322. doi: 10.1007/bf01323458

CHAVES, M. M. (1991). Effects of Water Deficits on Carbon Assimilation. *Journal of Experimental Botany, 42*(1), 1-16. doi: 10.1093/jxb/42.1.1

Chaves, M. M., Maroco, J., & Pereira, J. (2003). Understanding plant responses to drought — from genes to the whole plant. *Functional Plant Biology, 30*(3), 239-264. doi: http://dx.doi.org/10.1071/FP02076

Chen, Q., Baldocchi, D., Gong, P., & Dawson, T. (2008). Modeling radiation and photosynthesis of a heterogeneous savanna woodland landscape with a hierarchy of model complexities. [Article]. *Agricultural and Forest Meteorology, 148*(6-7), 1005-1020. doi: 10.1016/j.agrformet.2008.01.020

Cho, M. A. (2007). *Hyperspectral Remote Sensing of Biophysical Parameters* Wageningen Universiteit.

Collatz, G. J., Ball, J. T., Grivet, C., & Berry, J. A. (1991). Physiological and environmental regulation of stomatal conductance, photosynthesis and transpiration: a model that includes a laminar boundary layer. *Agricultural and Forest Meteorology, 54*(2–4), 107-136. doi: http://dx.doi.org/10.1016/0168-1923(91)90002-8

Combal, B., Baret, F., & Weiss, M. (2002). Improving canopy variables estimation from remote sensing data by exploiting ancillary information. Case study on sugar beet canopies. [Article]. *Agronomie, 22*(2), 205-215. doi: 10.1051/agro:2002008

Combal, B., Baret, F., Weiss, M., Trubuil, A., Mace, D., Pragnere, A., Myneni, R., Knyazikhin, Y., & Wang, L. (2003). Retrieval of canopy biophysical variables from bidirectional reflectance - Using prior information to solve the ill-posed inverse problem. [Article]. *Remote Sensing of Environment, 84*(1), 1-15. doi: 10.1016/s0034-4257(02)00035-4

Combes, D., Chelle, M., Sinoquet, H., & Varlet-Grancher, C. (2008). Evaluation of a turbid medium model to simulate light interception by walnut trees (hybrid NG38 x RA and Juglans regia) and sorghum canopies (Sorghum bicolor) at three spatial scales. [Article; Proceedings Paper]. *Functional Plant Biology, 35*(9-10), 823-836. doi: 10.1071/fp08059

Darvishzadeh, R., Skidmore, A., Schlerf, M., & Atzberger, C. (2008(a)). Inversion of a radiative transfer model for estimating vegetation LAI and chlorophyll in a heterogeneous grassland. *Remote Sensing of Environment, 112*(5), 2592-2604. doi: 10.1016/j.rse.2007.12.003

Darvishzadeh, R., Skidmore, A., Schlerf, M., Atzberger, C., Corsi, F., & Cho, M. (2008(b)). LAI and chlorophyll estimation for a heterogeneous grassland using hyperspectral measurements.

ISPRS Journal of Photogrammetry and Remote Sensing, 63(4), 409-426. doi: http://dx.doi.org/10.1016/j.isprsjprs.2008.01.001

dePury, D. G. G., & Farquhar, G. D. (1997). Simple scaling of photosynthesis from leaves to canopies without the errors of big-leaf models. [Article]. *Plant Cell and Environment, 20*(5), 537-557. doi: 10.1111/j.1365-3040.1997.00094.x

Destouni, G., Darracq, A., JarsjO, J., Prieto, C., & Shibuo, Y. (2009). Evapotranspiration in a warming climate: Model uncertainty and role for climate adaptation. *IOP Conference Series: Earth and Environmental Science, 6*(5), 052014.

Farquhar, G. D., Caemmerer, S. V., & Berry, J. A. (1980). A biochemical-model of photosynthetic co2 assimilation in leaves of c-3 species. [Article]. *Planta, 149*(1), 78-90. doi: 10.1007/bf00386231

Fernandes, R., Butson, C., Leblanc, S., & Latifovic, R. (2003). Landsat-5 TM and Landsat-7 ETM+ based accuracy assessment of leaf area index products for Canada derived from SPOT-4 VEGETATION data. *Canadian Journal of Remote Sensing, 29*(2), 241-258.

French, A. N., Hunsaker, D., Thorp, K., & Clarke, T. (2009). Evapotranspiration over a camelina crop at Maricopa, Arizona. *Industrial Crops and Products, 29*(2–3), 289-300. doi: 10.1016/j.indcrop.2008.06.001

Gastellu-Etchegorry, J., Gascon, F., & Esteve, P. (2003). An interpolation procedure for generalizing a look-up table inversion method. [Article]. *Remote Sensing of Environment, 87*(1), 55-71. doi: 10.1016/s0034-4257(03)00146-9

Goel, N. S., & Thompson, R. L. (2000). A snapshot of canopy reflectance models and a universal model for the radiation regime. *Remote Sensing Reviews, 18*(2-4), 197-225. doi: 10.1080/02757250009532390

Goudriaan, J. (1977). *Crop micrometeorology : a simulation study.* Proefschrift Wageningen, Pudoc, Wageningen. Retrieved from http://edepot.wur.nl/166537

Haile, A. (2005). *Integrating hydrodynamic models and high resolution DEM (LIDAR) for flood modelling.* M.Sc Master of science, Faculty of Geo-Informaytion Science and Earth Observation, Enschede, the Netherlands. Retrieved from http://www.itc.nl/library/papers_2005/msc/wrem/haile.pdf

Howell, T. A., Steiner, J. L., Schneider, A. D., Evett, S. R., & Tolk, J. A. (1997). Seasonal and maximum daily evapotranspiration of irrigated winter wheat, sorghum, and corn - Southern High Plains. [Article]. *Transactions of the Asae, 40*(3), 623-634.

Huber, S., Kneubühler, M., Psomas, A., Itten, K., & Zimmermann, N. E. (2008). Estimating foliar biochemistry from hyperspectral data in mixed forest canopy. *Forest Ecology and Management, 256*(3), 491-501. doi: 10.1016/j.foreco.2008.05.011

Ito, A. (2011). A historical meta-analysis of global terrestrial net primary productivity: are estimates converging? *Global Change Biology, 17*(10), 3161-3175. doi: 10.1111/j.1365-2486.2011.02450.x

Jacquemoud, S., Bacour, C., Poilve, H., & Frangi, J. P. (2000). Comparison of four radiative transfer models to simulate plant canopies reflectance: Direct and inverse mode. [Article]. *Remote Sensing of Environment, 74*(3), 471-481. doi: 10.1016/s0034-4257(00)00139-5

Jacquemoud, S., & Baret, F. (1990). PROSPECT a model of leaf optical properties spectra [Article]. *Remote Sensing of Environment, 34*(2), 75-91. doi: 10.1016/0034-4257(90)90100-z

Jacquemoud, S., Baret, F., Andrieu, B., Danson, F. M., & Jaggard, K. (1995). Extraction of vegetation biophysical parameters by inversion of the PROSPECT plus SAIL models on sugar beet canopy reflectance data applicationto TM and AVIRIS sensors. [Extr]. *Remote Sensing of Environment, 52*(3), 163-172. doi: 10.1016/0034-4257(95)00018-v

Jacquemoud, S., Verhoef, W., Baret, F., Bacour, C., Zarco-Tejada, P. J., Asner, G. P., Francois, C., & Ustin, S. L. (2009). PROSPECT plus SAIL models: A review of use for vegetation characterization. [Article; Proceedings Paper]. *Remote Sensing of Environment, 113*, S56-S66. doi: 10.1016/j.rse.2008.01.026

Ju, W., Wang, S., Yu, G., Zhou, Y., & Wang, H. (2010). Modeling the impact of drought on canopy carbon and water fluxes for a subtropical evergreen coniferous plantation in southern China

through parameter optimization using an ensemble Kalman filter. *Biogeosciences, 7*(3), 845-857.

Kobayashi, H., Baldocchi, D. D., Ryu, Y., Chen, Q., Ma, S. Y., Osuna, J. L., & Ustin, S. L. (2012). Modeling energy and carbon fluxes in a heterogeneous oak woodland: A three-dimensional approach. [Article]. *Agricultural and Forest Meteorology, 152*, 83-100. doi: 10.1016/j.agrformet.2011.09.008

Kull, O., & Kruijt, B. (1999). Acclimation of photosynthesis to light: a mechanistic approach. *Functional Ecology, 13*(1), 24-36. doi: 10.1046/j.1365-2435.1999.00292.x

Mäkelä, A., Hari, P., Berninger, F., Hänninen, H., & Nikinmaa, E. (2004). Acclimation of photosynthetic capacity in Scots pine to the annual cycle of temperature. *Tree Physiology, 24*(4), 369-376. doi: 10.1093/treephys/24.4.369

Medlyn, B. (2004). *A MAESTRO retrospective*. Cambridge: Cabi Publishing.

Meroni, M., Colombo, R., & Panigada, C. (2004). Inversion of a radiative transfer model with hyperspectral observations for LAI mapping in poplar plantations. [Article]. *Remote Sensing of Environment, 92*(2), 195-206. doi: 10.1016/j.rse.2004.06.005

Miller, J., Berger, M., Goulas, Y., Jacquemoud, S., Louis, J., Mohammed, G. M., N., Moreno, J., Moya, I., Perdos, R., Verhoef, W., & Zarco-Tejada, P. J. (2005). Development of a vegetation Fluorscence Canopy Model (Vol. 138 pp.): European space agency.

Monteith, J. L. (1981). Evaporation and surface temperature. *Quarterly Journal of the Royal Meteorological Society, 107*(451), 1-27. doi: 10.1002/qj.49710745102

Olioso, A., Soria, G., Sobrino, J., & Duchemin, B. (2007). Evidence of low land surface thermal infrared emissivity in the presence of dry vegetation. *IEEE Geosci Remote Sens Lett, 4*(1), 112-116. doi: 10.1109/lgrs.2006.885857

Qi, J., Kerr, Y. H., Moran, M. S., Weltz, M., Huete, A. R., Sorooshian, S., & Bryant, R. (2000). Leaf area index estimates using remotely sensed data and BRDF models in a semiarid region. [Article]. *Remote Sensing of Environment, 73*(1), 18-30. doi: 10.1016/s0034-4257(99)00113-3

Schlerf, M., & Atzberger, C. (2006). Inversion of a forest reflectance model to estimate structural canopy variables from hyperspectral remote sensing data. [Article]. *Remote Sensing of Environment, 100*(3), 281-294. doi: 10.1016/j.rse.2005.10.006

Schlerf, M., Atzberger, C., Hill, J., Buddenbaum, H., Werner, W., & Schüler, G. (2010). Retrieval of chlorophyll and nitrogen in Norway spruce (Picea abies L. Karst.) using imaging spectroscopy. *International Journal of Applied Earth Observation and Geoinformation, 12*(1), 17-26. doi: 10.1016/j.jag.2009.08.006

Shabanov, N. V., Huang, D., Yang, W. Z., Tan, B., Knyazikhin, Y., Myneni, R. B., Ahl, D. E., Gower, S. T., Huete, A. R., Aragao, L., & Shimabukuro, Y. E. (2005). Analysis and optimization of the MODIS leaf area index algorithm retrievals over broadleaf forests. *Ieee Transactions on Geoscience and Remote Sensing, 43*(8), 1855-1865. doi: 10.1109/tgrs.2005.852477

Shifa, Y. (2011). *Estimation of evapotranspiration using advection aridity approach.* M.Sc., Geo-information Science and Eart Observation, Twente, Enschede, The Netherlands. Retrieved from http://www.itc.nl/library/papers_2011/msc/wrem/shifa.pdf

Shuttleworth, W. J., & Wallace, J. S. (1985). Evaporation from sparse crops-an energy combination theory. *Quarterly Journal of the Royal Meteorological Society, 111*(469), 839-855. doi: 10.1002/qj.49711146910

Sinclair, T. R., Murphy, C. E., & Knoerr, K. R. (1976). Development and evaluation of simplified models for simulation canopy photosynthesis and transpiration. [Article]. *Journal of Applied Ecology, 13*(3), 813-829. doi: 10.2307/2402257

Sobrino J. A., Jimenez-Munoz J. C., Hidalgo V., Barella-Ortiz A., Soria G., Romaguera M., & B., F. (2008). Temperature and emissivity from AHS data in the framework of the AgriSAR and EAGLE campaigns. ESA Proceedings, AGRISAR and EAGLE Final Workshop: ESTECNoordwijk,.

Sobrino, J. A., Jiménez-Muñoz, C., Zarco-Tejada, J., Sepulcre-Cantó, G., & de Miguel, E. (2006). Land surface temperature derived from airborne hyperspectral scanner thermal infrared data. *Remote Sensing of Environment, 102*(1–2), 99-115. doi: 10.1016/j.rse.2006.02.001

Sobrino, J. A., Jimenez-Munoz, J. C., Zarco-Tejada, P. J., Sepulcre-Canto, G., & de Miguel, E. (2006). Land surface temperature derived from airborne hyperspectral scanner thermal infrared data. [Article]. *Remote Sensing of Environment, 102*(1-2), 99-115. doi: 10.1016/j.rse.2006.02.001

Steeneveld, G. J., KNMI., & Instituut, K. N. M. (2002). *On Photosynthesis Parameters for the A-gs Surface Scheme for High Vegetation*: Koninklijk Nederlands Meteorologisch Instituut.

Su, Z., Timmermans, W., Gieske, A., Jia, L., Elbers, J. A., Olioso, A., Timmermans, J., Van Der Velde, R., Jin, X., Van Der Kwast, H., Nerry, F., Sabol, D., Sobrino, J. A., Moreno, J., & Bianchi, R. (2008). Quantification of land–atmosphere exchanges of water, energy and carbon dioxide in space and time over the heterogeneous Barrax site. *International Journal of Remote Sensing, 29*(17-18), 5215-5235. doi: 10.1080/01431160802326099

Suits, G. H. (1971). The calculation of the directional reflectance of a vegetative canopy. *Remote Sensing of Environment, 2*(0), 117-125. doi: 10.1016/0034-4257(71)90085-x

Timmermans, J. (2011). *coupling optical and thermal directional radiative transfer to biophysical processes in vegetation canopies.* PhD thesis. Retrieved from http://www.itc.nl/library/papers_2011/phd/timmermans.pdf

Timmermans, J., & van der Tol, C. (2012). *REFLEX 2012 Regional Experiments For Land-atmosphere Exchanges*.

van der Tol, C., Verhoef, W., Timmermans, J., Verhoef, A., & Su, Z. (2009). An integrated model of soil-canopy spectral radiances, photosynthesis, fluorescence, temperature and energy balance. [Article]. *Biogeosciences, 6*(12), 3109-3129.

Verhoef, W. (1984). Light scattering by leaf layers with application to canopy reflectance modeling: The SAIL model. *Remote Sensing of Environment, 16*(2), 125-141. doi: 10.1016/0034-4257(84)90057-9

Verhoef, W. (2012). *Atmospheric correction of airborne data*. Water Resources department. Faculty of Geo-Information Science and Earth Observation (ITC), University of Twente. Enschede, The Netherlands.

Verhoef, W., Jia, L., Xiao, Q., & Su, Z. (2007). Unified optical-thermal four-stream radiative transfer theory for homogeneous vegetation canopies. [Article]. *Ieee Transactions on Geoscience and Remote Sensing, 45*(6), 1808-1822. doi: 10.1109/tgrs.2007.895844

Walthall, C., Dulaney, W., Anderson, M., Norman, J., Fang, H. L., & Liang, S. L. (2004). A comparison of empirical and neural network approaches for estimating corn and soybean leaf area index from Landsat ETM+ imagery. [Article; Proceedings Paper]. *Remote Sensing of Environment, 92*(4), 465-474. doi: 10.1016/j.rse.2004.06.003

Wandera, L. (2011). *Mapping chlorophyll concentration in a mangrove forest by model inversion approach applied to hyperspectral imagery* Master of Science, Twente, Academic output. Retrieved from http://www.itc.nl/library/papers_2011/msc/nrm/wandera.pdf (44)

Wang, Y. P., & Jarvis, P. G. (1990). Influence of crown structural propoerties on PAR absorpation, photosynthesis and transpiration in sitka spruce application of a model (MAESTRO). [Article; Proceedings Paper]. *Tree Physiology, 7*(1-4), 297-316.

Wang, Y. P., & Leuning, R. (1998). A two-leaf model for canopy conductance, photosynthesis and partitioning of available energy I: Model description and comparison with a multi-layered model. [Article]. *Agricultural and Forest Meteorology, 91*(1-2), 89-111. doi: 10.1016/s0168-1923(98)00061-6

Wang, Y. P., Tian, Y., Zhang, Y., El-Saleous, N., Knyazikhin, Y., Vermote, E., & Myneni, R. (2001). Investigation of product accuracy as a function of input and model uncertainties: Case study with SeaWiFS and MODIS LAI/FPAR algorithm. *Remote Sensing of Environment, 78*(3), 299-313. doi: http://dx.doi.org/10.1016/S0034-4257(01)00225-5

Weiss, M., & Baret, F. (1999). Evaluation of canopy biophysical variable retrieval performances from the accumulation of large swath satellite data. [Article]. *Remote Sensing of Environment, 70*(3), 293-306. doi: 10.1016/s0034-4257(99)00045-0

Weiss, M., Baret, F., Myneni, R. B., Pragnere, A., & Knyazikhin, Y. (2000). Investigation of a model inversion technique to estimate canopy biophysical variables from spectral and directional reflectance data. [Article]. *Agronomie, 20*(1), 3-22.

Wetzel, P. J., & Chang, J.-T. (1988). Evapotranspiration from Nonuniform Surfaces: A First Approach for Short-Term Numerical Weather Prediction. *Monthly Weather Review, 116*(3), 600-621. doi: 10.1175/1520-0493(1988)116<0600:efnsaf>2.0.co;2

Williams, G. (2012). *Estimating chlorophyll content in a mangrove forest using a neighbourhood based inversion approach.* MSc, university of Twente, Enschede, The Netherland.

Wolf, A., Akshalov, K., Saliendra, N., Johnson, D. A., & Laca, E. A. (2006). Inverse estimation of Vcmax, leaf area index, and the Ball-Berry parameter from carbon and energy fluxes. *Journal of Geophysical Research: Atmospheres, 111*(D8), n/a-n/a. doi: 10.1029/2005jd005927

Wu, C., Niu, Z., Tang, Q., & Huang, W. (2008). Estimating chlorophyll content from hyperspectral vegetation indices: Modeling and validation. *Agricultural and Forest Meteorology, 148*(8–9), 1230-1241. doi: http://dx.doi.org/10.1016/j.agrformet.2008.03.005

Wullschleger, S. D. (1993). Biochemical limitations to carbon assimilation in c(3) plants - a retrospective analysis of the A/CI curves from 109 species. *Journal of Experimental Botany, 44*(262), 907-920. doi: 10.1093/jxb/44.5.907

Xu, L., & Baldocchi, D. D. (2003). Seasonal trends in photosynthetic parameters and stomatal conductance of blue oak (Quercus douglasii) under prolonged summer drought and high temperature. *Tree PhysioI, 23*(13), 865-877. doi: 10.1093/treephys/23.13.865

Yang, W., Shabanov, N. V., Huang, D., Wang, W., Dickinson, R. E., Nemani, R. R., Knyazikhin, Y., & Myneni, R. B. (2006). Analysis of leaf area index products from combination of MODIS Terra and Aqua data. *Remote Sensing of Environment, 104*(3), 297-312. doi: 10.1016/j.rse.2006.04.016

Young, K. J., & Long, S. P. (2000). Crop ecosystem responses to climatic change: maize and sorghum. In K. R. Reddy & H. F. Hodges (Eds.), *Climate change and global crop productivity* (pp. 107-131). Wallingford: CABI.

Yuanliu, X., Runsheng, W., Shengwei, L., Suming, Y., & Bokun, Y. (2008). *Atmospheric correction of hyperspectral data using MODTRAN model*. Paper presented at the Remote Sensing of the Environment, China. http://www.ewp.rpi.edu/hartford/users/papers/engr/ernesto/brazw/Project/Other/Research/Soot/Yuanliu_MODTRANAtmosCorrection.pdf

Zarco-Tejada, P. J., & Sepulcre-Cantó, G. (2007). Remote sensing of vegetation biophysical parameters for detecting stress condition and land cover changes. *Estudios de la Zona No Saturada del Suelo, VIII*, 8.

Zhan, X., Kustas, W. P., & Humes, K. S. (1996). An intercomparison study on models of sensible heat flux over partial canopy surfaces with remotely sensed surface temperature. *Remote Sensing of Environment, 58*(3), 242-256. doi: http://dx.doi.org/10.1016/S0034-4257(96)00049-1

Zhang, R. (2010). *Estimation of land-atmosphere carbon exchange, combining remote sensing, modelling and CO2 flux data* MSc, Edinburgh Retrieved from http://www.google.nl/search?hl=en&tbo=d&noj=1&spell=1&q=inverse+estimation+of+Vmax+,+leaf+areas+index+and+the+Ball+Berry+parameter+from+carbon+and+energy+fluxes&sa=X&ei=yiwGUZ_3GsSx0AXaqIHABw&ved=0CCsQvwUoAA&biw=1360&bih=596

Zhou, D. K., Larar, A. M., Xu, L., Smith, W. L., Strow, L. L., Ping, Y., Schlu, x, ssel, P., & Calbet, X. (2011). Global land surface emissivity retrieved from satellite ultraspectral IR measurements. *Geoscience and Remote Sensing, IEEE Transactions on, 49*(4), 1277-1290. doi: 10.1109/tgrs.2010.2051036